Review

Carlo Danieli*, Alexei Andreanov, Daniel Leykam and Sergej Flach

Flat band fine-tuning and its photonic applications

Abstract: Flat bands – single-particle energy bands – in tight-binding lattices, aka networks, have attracted attention due to the presence of macroscopic degeneracies and their sensitivity to perturbations. They support compact localized eigenstates protected by destructive interference. This makes them natural candidates for emerging exotic phases and unconventional orders. In this review we consider the recently proposed systematic ways to construct flat band networks based on symmetries or fine-tuning. We then discuss how the construction methods can be further extended, adapted or exploited in presence of perturbations, both single-particle and many-body. This strategy has lead to the discovery of non-perturbative metal-insulator transitions, fractal phases, nonlinear and quantum caging and many-body nonergodic quantum models. We discuss what implications these results may have for the design of fine-tuned nanophotonic systems including photonic crystals, nanocavities, and metasurfaces.

Keywords: photonic lattices; flat band; compact localized states; fine-tuning; localization of light; nonlinear regime

---

*Corresponding author: Carlo Danieli, Institute for Complex Systems, National Research Council (ISC-CNR), Via dei Taurini 19, 00185 Rome, Italy, E-mail: carlo.danieli87@gmail.com.
https://orcid.org/0009-0004-1370-9462
Alexei Andreanov, Center for Theoretical Physics of Complex Systems, Institute for Basic Science (IBS), 34126, Daejeon, Republic of Korea; and Basic Science Program, Korea University of Science and Technology (UST), Daejeon 34113, Republic of Korea, E-mail: aalexei@ibs.re.kr.
https://orcid.org/0000-0002-3033-0452
Daniel Leykam, Centre for Quantum Technologies, National University of Singapore, 3 Science Drive 2, Singapore 117543, Singapore, E-mail: daniel.leykam@gmail.com.
https://orcid.org/0000-0002-8588-9886
Sergej Flach, Center for Theoretical Physics of Complex Systems, Institute for Basic Science (IBS), 34126, Daejeon, Republic of Korea; Basic Science Program, Korea University of Science and Technology (UST), Daejeon 34113, Republic of Korea; and Centre for Theoretical Chemistry and Physics, The New Zealand Institute for Advanced Study, Massey University Auckland, Auckland, New Zealand, E-mail: sergejflach@googlemail.com

1 Introduction

Flat bands (FB) are strictly dispersionless bands embedded in a band structure of waves which in general can propagate through a spatially periodic medium [1]–[3].

We focus on lattices with finite range hopping, which vanishes exactly beyond some finite distance. In this case, flat band lattices are accompanied with the existence of compact localized eigenstates (CLS). In Figure 1(a) the two-dimensional Lieb lattice is shown with its CLS occupying four sites, as well as the corresponding band structure with two dispersive and flat bands in Figure 1(b). The CLS is an exact eigenstate of the system. Despite existing network connections to unoccupied sites the CLS resists any expansion due to destructive interference. Photonic realizations of this CLS and flat band example were reported by Vicencio et al. [4], Mukherjee et al. [5] and Xia et al. [6]. The authors used a femtosecond-laser writing on silica glass wavers to generate the Lieb lattice (Figure 1(c)), and successfully propagated light through the resulting photonic waveguide network in a compact localized state as shown in Figure 1(d).

The fascination in flat bands derives from the fact that a flat band results in macroscopic degeneracy and absence of transport, which – once broken, even slightly by tiny perturbations – result in novel transporting phases whose properties depend on the type of perturbations added. The perturbations hence become the game maker, and that is what turns flat bands into interesting starting points for switching between different phases of matter through tiny changes of tiny perturbations. Consequently, perturbation terms have to be controlled through meticulous fine-tuning. The same also applies to flat band lattices themselves, as they are part of manifolds and different flat band lattices respond differently to the same perturbation. Fine-tuning within these manifolds is therefore a desirable scheme which will allow for the above-mentioned switching.

The still-young field of flat band physics went through a few evolution cycles already. It probably first manifested through an observation of Bill Sutherland that compact localized eigenstates are not a prerogative of tight-binding models of quasicrystals [7], but persist also in systems with strict discrete translational invariance [8]. Then Elliott Lieb
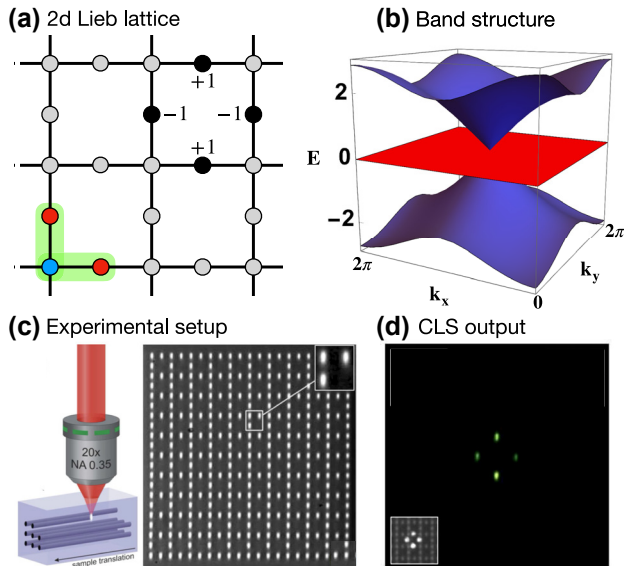
(a) 2d Lieb lattice

(b) Band structure

(c) Experimental setup

(d) CLS output

Figure 1: Flatband in the 2d Lieb lattice. (a) Lattice profile and lattice and the location of the CLS. Solid circles show the CLS profile with given amplitudes and alternating phases (indicated by the signs). The green shaded area indicates the unit cell, with the majority sublattice (red) and the minority sublattice (blue). (b) Band structure with the clearly visible flat band (red) between two dispersive bands (blue). (c) Femtosecond-laser writing technique on a silica glass wafer and microscope image at the output facet of a Lieb lattice for white light propagation. Reprinted with permission from Ref. [4], (d) output experimental pattern for an initial CLS excitation. The inset shows the input intensity profile [4].

Figure 2: The structure diagram of stacked and twisted bilayer graphene. Reprinted with permission from Ref. [14].[1]

used the Lieb lattice and its flat band for exciting high T_c superconductivity physics of charge transport in Co-O_2 planes on one side [9], but on the other side firmly introduced the concept of chiral symmetry protected FBs, see Figure 1. The first cycle was completed by Mielke [10] and Tasaki [11], with Mielke offering a flat band generator using line graphs, and Tasaki showing that the Lieb lattice FB can be preserved under specific well-chosen fine-tuned perturbations of the Lieb lattice. While both aimed at and described novel features of ground and excited states of an electronic many-body interacting system, we stress here their contribution to the first evolution cycle of the single particle FB physics field.

During the second cycle of about 20 years an impressive amount of publications – mainly theoretical – was added targeting condensed matter-related topics and questions [1]. Many aspects and details of FB properties were reported, and a number of qualitatively different properties were identified during this second cycle hinting at the existence of different classes of FBs. However, it was far from being clear how to systematically search for new flat band models even at the level of noninteracting single particle physics. This is mainly due to the condensed matter material science
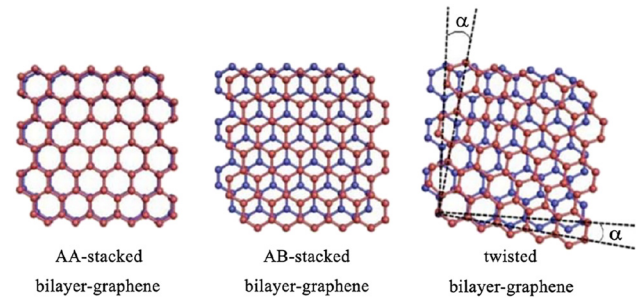
platform, which does not allow to easily prepare materials with fine-tuned electronic properties. It is interesting to note the hype following the introduction of magic angle twists of bilayer structures with graphene and other two-dimensional materials, see Figure 2. For small twist angles the moiré patterns lead to large effective unit cells with easily more than 50–100 sites and therefore corresponding bands in the band structure. For fine-tuned magic angles one or a few bands turn almost flat, potentially resulting in superconductivity below one Kelvin. While this is certainly an important and interesting phenomenon, it is far from the rigor of the flat band physics discussed here and its realization with highly flexible light based artificial material platforms. It is worth pointing to attempts connecting nearly flat bands in twisted bilayers to perfect flat bands [12], [13].

The third evolution cycle was ripe to start. It needed systematic and as complete as possible FB generators. The key was to use the CLS as a starting point rather than an outcome [15]. The next step in that direction successfully lead to the first and complete FB generator for one-dimensional two band lattices [16]. With that it was clear that flat band models are and can be obtained through fine-tuning [17]–[20]. That result opened the door for experimental platforms that can be accurately fine-tuned. Indeed classical condensed matter platforms are mostly using electronic and magnonic waves propagating in crystals and materials which lack fine-tuning potential, with the spatial periods having length scales of the order of Angstrom and were until recently way beyond the limits of direct *in-situ* observations [21], [22]. Instead, some of the most important emerging new photonic platforms are exploiting light propagation in structured media, or atomic Bose–Einstein condensates propagating in optical lattices generated by laser light, or light

and excitons hybridizing into polaritonic dissipative condensates and propagating in structured media while kept afloat with external laser light pumping [2], [3]. All these platforms are characterized by a high degree of tunability, and by length scales dictated by the wavelength of light, making direct *in-situ* observations and characterizations possible. For example, recent demonstrations of photonic moiré superlattices illustrate the ability to fabricate fine-tuned periodic structures with hundreds of elements per unit cell [23]–[26].

This review intends to give a broader view on the fine-tuning properties of flat bands, to discuss in more detail a number of recent fine-tuning results as well as outcomes of perturbing flat bands, and connect to recent or still to be performed experimental studies in the broader area of photonics and light–matter interaction.

2 Needles in the haystack

Spatially periodic tight-binding networks are models which describe the propagation of linear waves on a spatial lattice. The wave is described by a finite number ν of wave states in a spatial unit cell which is repeated periodically in space. Each local wave or mode state is characterized by a complex number – amplitude and phase, similar to an oscillator. These wave states are connected through hopping elements with other states and can tunnel (hop), as shown in Figure 3. Examples can be e.g. single mode optical waveguides carrying light which tunnels to nearby waveguides through its evanescent tails, among many others. In real physical space the evolution of these systems is modeled with a time-dependent Schrödinger equation $i\dot{\psi}_{l,\mu} = \sum H_{\{l,\mu\},\{m,\kappa\}}\psi_{m,\kappa}$ with $H_{\{l,\mu\},\{m,\kappa\}}$ being the matrix element of the Hamiltonian $\hat{\mathcal{H}}_{sp}$. Here l,m label the unit cells, and $1 \leq \mu, \kappa \leq \nu$ label the state inside one unit cell. The onsite energies (diagonal elements) are defined as $\epsilon_{l,\mu} = H_{\{l,\mu\},\{l,\mu\}}$, and the off-diagonal elements describe the hopping, often abbreviated by t (not to be confused with time). Time itself can be the physical time, or the propagation distance of light in the case of optical waveguides. Since we consider $\hat{\mathcal{H}}_{sp}$ to be invariant under discrete translations, application of Bloch's theorem and transformation into reciprocal space results in a Hamiltonian $\hat{\mathcal{H}}_{sp}(\vec{k})$. The number of allowed wave vectors $\vec{k}$ equals the number of unit cells, and $\hat{\mathcal{H}}_{sp}(\vec{k})$ is a $\nu \times \nu$ matrix. Its eigenvalues $E_\mu(\vec{k})$ form a Bloch band structure which is periodic in k-space. The normalized eigenvectors are coined the polarization vector field for each of the Bloch bands.

The networks are classified according to their spatial dimension d, the Bravais lattice structure which is formed
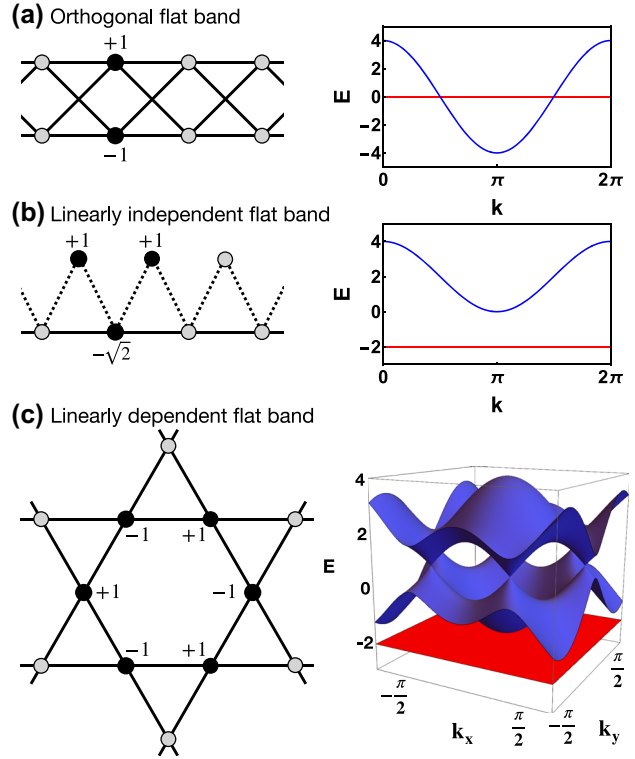

Figure 3: List of flat band types. (a) A 1d cross-stitch lattice with an orthogonal flat band. (b) A 1d sawtooth lattice with a linearly independent flat band. (c) A 2d Kagome lattice with a linearly dependent flat band. For all cases the left plots show the lattice structure and location of CLS. Solid circles show the CLS profile with given amplitudes and alternating phases (indicated by the signs). Right plots – corresponding band structure for each model (flat band is shown in red color).

by the unit cells, the number of Bloch bands ν (i.e. the minimal number of sites of the unit cell representation, or likewise the number of sublattices embedded into the Bravais lattice structure) and the hopping range m_c. Fixing these classifiers however still leaves the values of the hopping strengths and the onsite energies undefined, yielding a large dimensional manifold of tight-binding networks.

Without any further restrictions a typical band structure will consist of dispersive bands only. Viewing such a manifold of in general dispersive band structures as a haystack, the task of finding submanifolds of networks with flat bands in their band structure appears to be similar to the task of finding a needle in the haystack. We will discuss how this can be done systematically.

The choice of the hopping strengths and the onsite energies becomes crucial to ensure features to a lattice – e.g. local and global symmetries, topology, among others. Such a procedure of targeting certain features by properly selecting the hoppings and onsite energies, which may either

result in a specific lattice model or in sub-families (*manifolds*) of lattices, goes by the name of *fine-tuning*.

From a practical viewpoint the fine-tuning of a flat band network therefore is a careful adjusting of the hopping values and onsite energies of a tight-binding network in order to zero the dispersion of (at least) one of its Bloch bands: $E_\mu(\vec{k}) = E_\mu(\vec{k}')$ for any choice of the wave vectors. Identifying these fine-tuning conditions is equivalent to obtaining a flat band generator: fixing relevant classifiers as e.g. the desired dimension D, number of bands ν, and hopping range m_c of the lattice, *generate* the manifold of networks $\hat{\mathcal{H}}_{\text{sp}}$ which possess (at least) one flat band. If the flat band generator approach results in reliable predictions, they can be applied in the lab to fine-tune samples in order to obtain flat bands – e.g. see Ref. [27].

Making a network to possess certain global symmetries can be viewed on one hand as a special way of finetuning, and on the other hand as a way to ensure the existence of flat bands and CLSs without the need of expliticely proving their existence. Two known cases – chiral [28] and anti-parity-time [29] symmetries – are doing the job. Let us consider the chiral case, and use the 2D Lieb lattice in Figure 1(a) as an example. For chiral flat band lattices we need bipartite networks with all sites separated into sublattices A and B, such that sites from sublattice A are connected only to sites from sublattice B and vice versa, without any additional onsite energies. Eigenstates of such a network come in pairs with energy $\pm E$. We further request to have more sublattice A sites in a unit cell than sublattice B sites, making the A sublattice a so-called majority sublattice. In the Lieb lattice in Figure 1(a) the majority and minority sublattices are conlored in red and blue. In that case it follows [28] that there must be a macroscopic number (at least equal to the number of unit cells) of eigenstates with chiral energy $E = 0$, which therefore form a chiral flat band. It further follows that the eigenvectors are nonzero entirely on the majority sublattice, and that they can be cast into the form of CLSs. Adding hoppings which connect the minority sublattice sites and onsite energies on these sites will not affect the chiral flat band and its CLSs. Making all hoppings as well as the minority site energies random will not destroy the CLSs either. Shifting the majority onsite energies equally will also keep the CLSs and only shift the flat band energy [30].

3 Flat band types

For networks with finite hopping range $m_c < \infty$ and a finite number of bands $\nu < \infty$, a flat band results in the existence of a macroscopically degenerate set of compact localized eigenstates [34]. Enforcing the existence of compact

localized states in tight-binding networks yields an effective and systematic method for generating flat band. This approach calls for additional classifiers for flat bands in addition to the above-mentioned ones D, ν, m_c – namely the *size* U of a CLS (i.e. the number of occupied unit cells) and for $D \geq 2$ the *shape* (i.e. the arrangement of such U unit cells). Flat bands can be sorted into different classes of varying complexity, that largely define their response to perturbations. These classes are defined by the properties of the CLS set of a flat band: their *orthogonality* and *completeness*, i.e. *linear independence*. Further the classes differ by the result of a projection of an arbitrary state on the FB state space, i.e. by the so-called real space projector. Finally FBs from different classes respond differently to the action of local unitaries, i.e. unitary transformations of the unit cell (and subsequent local unitaries after redefining the unit cell). The simplest class consists of *orthogonal flat bands* [15], whose set of CLS is complete and orthonormal. An example is the cross-stitch lattice (see Figure 3(a)), which has been experimentally realized in Refs. [35]–[37]. In this case, real space projectors onto the flat band Hilbert space are strictly compact [38], [39]. Local unitaries can completely detangle the FB and its CLSs from the rest of the network, i.e. they can result in a diagonalization of the FB part using strictly local transformations, without the need to transform into k-space [15]. Next is the class of *linearly independent flat bands* with a complete and linearly independent but non-orthogonal set of CLS. An example is the sawtooth lattice [40] (see Figure 3(b)), experimentally realized in Ref. [41]. For this class, there is no *local* unitary transformation that can make the CLS set orthogonal. The real space projector for linearly independent flat bands is decaying exponentially in space. A detangling procedure is not applicable for this class. Finally, there are *linearly dependent flat bands* whose CLS sets are neither orthogonal nor complete, but linearly dependent. An example of this class is the Kagome lattice [9] (see Figure 3(c)) which has been experimentally realized in Ref. [42]. Linearly dependent flat bands exist only in dimension $d \geq 2$, and are touching at least one dispersive band at a special k point. Their real space projector is decaying algebraically as $1/r^d$ [43]–[45]. Such bands are also referred to as critical or singular [46], [47], since their polarisation vector in the Bloch space vanishes in some point in the Brillouin zone, indicating a band touching. Conversely, all the flat bands with polarisation vectors that are nonzero everywhere in the Brillouin zone, e.g. with complete sets of CLS [46], are called non-singular. Further experimental photonic realizations of the three types of flat bands were reported in Refs. [31]–[33] and are shown in Figure 4.

A particular type of networks hosts a finite number of bands with all bands flat (ABF). Flat bands from ABF
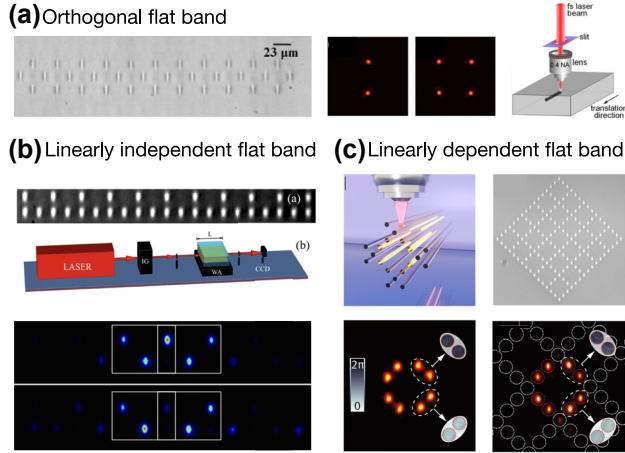
(a) Orthogonal flat band

(b) Linearly independent flat band   **(c)** Linearly dependent flat band

Figure 4: Experimental realizations of samples of the three types of flat bands. (a) A 1d rhombic lattice with an orthogonal flat band. Reprinted with permission from Ref. [31] © Optical Society of America. (b) A 1d Stub lattice with a linearly independent flat band. Reprinted with permission from Ref. [32]. (c) A 2d decorated Lieb lattice with a linearly dependent flat band. Reprinted with permission from Ref. [33].

(a)   **(c)**

(b) $\phi = \pi$ **(d)**

Figure 5: All bands flat diamond chain. (a) Diamond chain profile with magnetic flux ϕ (dashed complex hoppings). (b) CLS profiles for the all bands flat with flux value $\phi = \pi$ and three flat bands at $E = 0$ and $E = \pm 2$. (c) Simplified sketch illustrating the waveguide paths of a photonic diamond chain with $\phi = \pi$ flux per plaquette realized by circularly curving the lattice. Reprinted with permission from Ref. [52]. (d) Experimentally measured output intensity distributions at two different propagation distances. Reprinted with permission from Ref. [52].

lattices fall into the first class of orthogonal ones [48], [49]. Since all bands lack dispersion, there is no transport in an ABF network. Consequently any local initial state will not be able to propagate beyond a certain finite distance. Early realizations were theoretically obtained by Vidal et al. [50], [51] through adding a magnetic flux to a bipartite flat band lattice with the flat band at energy $E = 0$ being protected by chirality [28]. The flux only modifies the hoppings, preserves the chiral symmetry, and keeps the $E = 0$ band flat. An example is shown in Figure 5(a) for the diamond chain. At the magic flux value $\phi = \pi$ all other bands turn flat as well, resulting in an ABF lattice with flat band energies $E = 0, \pm 2$ (in units of the hopping strength). The CLS profiles are shown in Figure 5(b). Experimental photonic realizations of fluxes and ABF lattices were obtained by Mukherjee et al. [52] with the help of circularly curved laser-imprinted photonic waveguides (Figure 5(c)). Careful tuning to the magic flux value $\phi = \pi$ allowed to observe absence of dispersion and complete localization and trapping of a locally injected light excitation as shown in Figure 5(d). Other experimental realizations of ABF lattices in photonic lattices include [53]–[55].

The choice of flat band classifiers has a strong impact on the features of both the set of CLSs and the overall band structure. The amplitudes of the encoded CLS profile become the knobs of generator schemes, as tuning such entries yields different flat band networks. The resulting parametrization scheme of flat band networks is exhaustive and applicable in any dimension D and for any finite
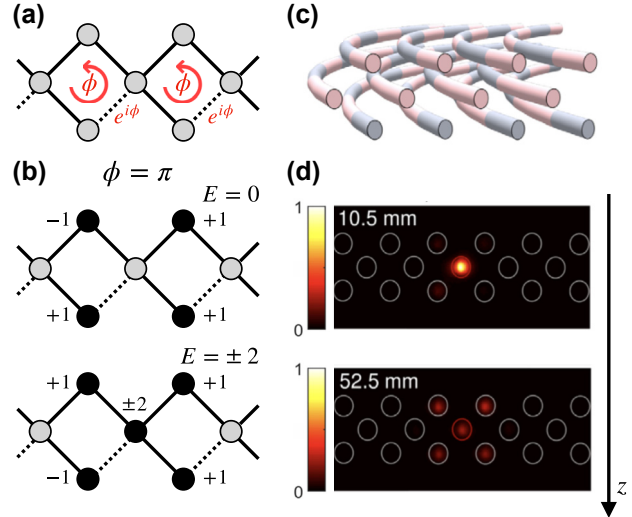
number of bands ν. It further provides a useful tool to study and control the impact of perturbations.

4 Tuning and detuning

The needle in the haystack – the flat band manifold – has a surprising internal fine structure. Properly identifying this manifold substructure promises to observe novel transport regimes which emerge from perturbations of different flat band submanifolds. Even if the perturbation is the same, the outcome can be expected to differ qualitatively depending on the submanifold it is applied to.

4.1 Tuning

To achieve fine tuning – or simply tuning – is synonymous to finding a generator procedure which has flat band network models on output. What sets different generators apart is not only the algorithm itself, but also the parameters which need to be specified on input.

An early documented attempt is the line graph generator of Mielke [10] designed to tackle flat band ferromagnetism in Hubbard models. On input one chooses a tight binding network with some dispersive band structure which does not contain a flat band. One then constructs the line graph of this network. It is obtained by replacing bonds
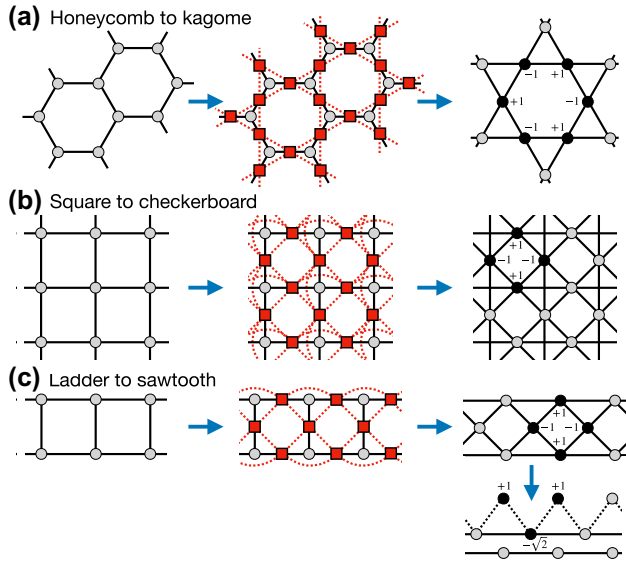
Figure 6: Line graph constructions of the kagome lattice from the honeycomb lattice (a), of the checkerboard lattice from the square lattice (b), and the sawtooth chain from the two legs ladder (c).

by new sites, and new bonds (all of the same amplitude) between all new sites whose old bonds shared a joint old site. The line graph is a new tight binding network which possesses one flat band as the lowest energy band in the band structure (or highest, depending on the new bond strength sign) [10]. It was mainly studied and applied in two dimensions. Examples are the line graph of the honeycomb lattice which is the kagome lattice (Figure 6(a)), and the square lattice maps into the checkerboard lattice (Figure 6(b)). But this construction works also in one dimension, where e.g. a simple two leg ladder will map onto a three band lattice with up down symmetry and one band flat (Figure 6(c)). An additional simple transformation into symmetric and antisymmetric up-down cooridinates finally transforms the line graph into a sawtooth lattice and a decoupled chain. This line graph generator does not contain continuous free parameters, thus it generates a countable set of flat band networks only. Further the flat band is always located at the extreme of the band structure.

Another early achievement was due to Tasaki [11]. While mainly focusing on flat band ferromagnetism aspects due to many-body interactions, this work studied the consequences of decorating the known 2D Lieb flat band lattice (Figure 1) with next to nearest neighbour hoppings between minority sublattice sites as shown in Figure 7(a). As discussed above, this modification destroys the chiral symmetry, yet preserves the flat band at $E = 0$ with its unchanged CLS. Since the chirality is broken, we can expect that the two dispersive bands open a gap between each other, and cease
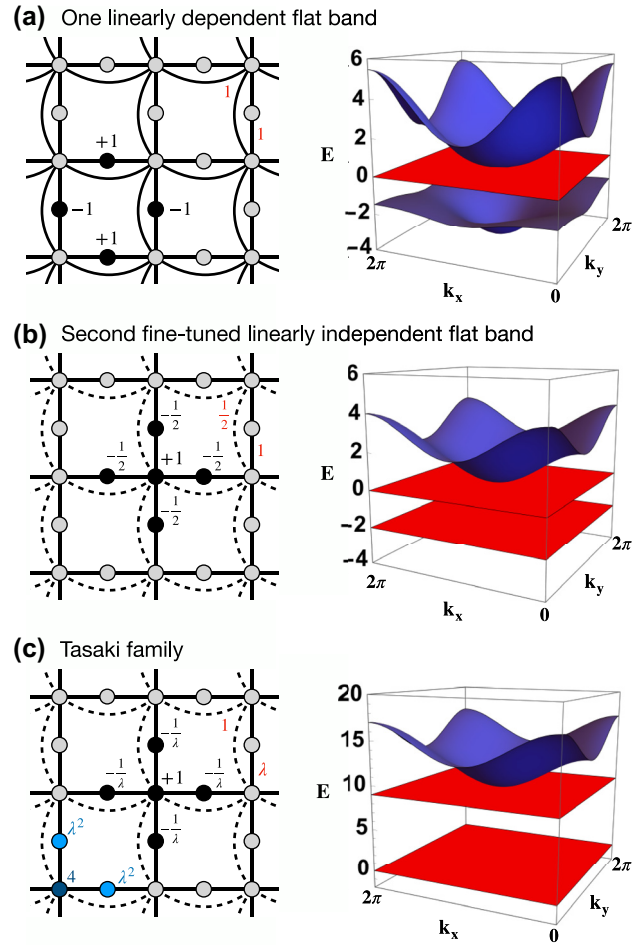

Figure 7: The Tasaki construction of flat bands in the 2d Lieb. (a) Decorated 2d Lieb (left) with uniform hopping strengths. Solid circles show the CLS profile with given amplitudes and alternating phases (indicated by the signs). Band structure (right) with one flat band (red) band touching the upper dispersive band (blue) and gapped away from the lower dispersive band (blue). (b) Same as (a) with fine-tuned next nearest neighbor hopping to 1/2. Solid circles show the CLS profile corresponding to the second flat band at $E = -2$. (c) Tasaki family (left) with parametric hopping λ (solid line) and onsite energies (blue colored circles). Band structure (right) with two flat bands (red) and a dispersive band (blue) for $\lambda = 3$.

to be symmetry related copies of each other. However the CLS of the flat band is unchanged – therefore the CLS set must still be linearly dependent! From that we conclude that the flat band at $E = 0$ must still touch one of the dispersive bands, as confirmed in Figure 7(a). A further surprise comes when choosing the additional hoppings to be half of the original Lieb hoppings. In that case lower dispersive band turns into a second flat band. It is supported by a new CLS in Figure 7(b). Tasaki also added and finetuned onsite energies and managed to obtain a flat band network for which the new ground state flat band is supported by tunable CLS sets

as shown in Figure 7(c). The main conclusion then is that flat band networks have to be finetuned on the one hand with respect to their network parameters, but form continuous manifolds on the other hand with some tuning and navigating manifold parameters which smoothly change the CLS details. This insight culminates in the discovery of flat band generators which are based on the properties of tunable CLS sets to be supported.

CLS based generators for orthogonal flat bands have been reported in Ref. [15]. They harvest on the existence of local unitary operations (one per each unit cell) which completely detangle the CLSs into uncoupled single sites in the new basis. Inverting this detangling procedure generates tunable families of flat band networks. One therefore starts with a choice of some dispersive tight binding network, adds one or more decoupled sites (at possibly one or more different onsite energies) to each unit cell, and then applies the local unitaries. In Figure 8(a) we schematically show this detangling-entangling procedure for a 1D two bands problem with one flat band. The free parameters are the angles of the local unitary transformation. In addition one can redefine the unit cell and perform another tunable unitary procedure. The resulting CLS will also continuously depend on the tuning parameters, and increase in size the more redefined unit cells are used. Still both the CLS set stays orthonormal, and the flat band energies are kept unchanged. The procedure works in any lattice dimension, for any lattice to start with. To generate ABF networks one has to only choose a Bravais lattice, the number of flat bands and their flat band energies. Each Bravais lattice point is then initially containing only uncoupled sites at their own onsite energies, one per flat band. Then one performs at least two sets of local unitary operations (in 1D, more are required in higher dimensions) with different unit cell choices to arrive at a fully connected network, yet with all bands flat [48], [56] as shown in Figure 8(b). Early studies of Vidal et al. [50], [51] as well as later ones by Brosco et al. [57] added magnetic fluxes to chiral flat band networks and observed that at particular values of the flux all bands turn flat, which was coined Aharonov–Bohm caging. It follows that there is no need to introduce first a magnetic flux and then to finetune this flux value to arrive at ABF networks. Instead one can simply follow the above local unitary approach to arrive at the most complete ABF generator.

CLS based generators for non-orthogonal but in general linearly independent flat bands are the most involved ones. To succeed, one needs to first choose a particular CLS and a particular network class with still free hopping strength parameters – as schematically represented in the
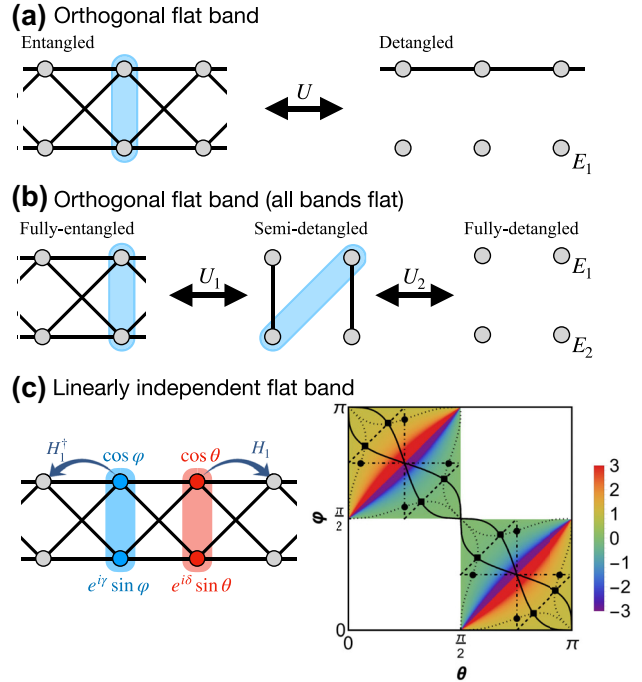

Figure 8: 1d flat bands generator schemes. (a) Entangling procedure for lattices supporting one dispersive band and one flat band with orthogonal CLS via local a unitary transformation within each unit cells (blue shaded area). (b) Same as (a) for all-band-flat network. (c) Left: Schematics of the compact localized state occupying two unit cells for a lattice with two bands and nearest neighbour unit cell hopping. The amplitudes and phases of the CLS components in each of the two unit cells are parametrized by four angles. Right: Flat band energy for two bands lattice as function of the parameterizing angles. The colored squares host FB networks, while the white ones do not (for nearest-neighboring hopping). The solid and dashed lines indicate diverse flat band sub-manifolds. Figure reprinted with permission from Ref. [16].

left panel of Figure 8(c). Second, one formulates hopping strength conditions for the destructive interference at the surface of the CLS. Finally, one needs to satisfy the hopping strength conditions on a finite network manifold of the size of the CLS which supports this CLS as an eigenstate. The corresponding algebraic equations which need to be solved are usually of nonlinear nature, which can complicate the task. For the simplest case of dimension $d = 1$, nearest unit cell hopping only, and two bands with one of them flat, the task can be accomplished in closed form analytically as shown by Maimaiti et al. [16]. Interestingly the entire family can be mapped onto 1D sawtooth networks Figure 3(b) with tunable hoppings and onsite energies. Two nontrivial free angles remain which navigate through the flat band family as shown in Figure 8(c) (colored areas). In particular, the solid and dashed lines indicate subfamilies of flat band networks with symmetry relations between hoppings and potentials. The upshot then is that indeed

tunable CLS sets lead to tunable flat band networks – the needle in the haystack has an enormous internal structure. Maimaiti et al. extended the generator method to 1D networks with more bands [17], as well as to 2D networks [18] confirming the above conclusions. The algebraic complexity quickly grows and calls for special ways to solve the resulting equations. Nonorthogonal flat band generators can be always combined with orthogonal flat band generators, either in order to complexify the resulting network structure even more, or in order to perform a partial detangling of a macroscopic fraction of CLSs for non-orthogonal flat bands [16].

In order to generate linearly dependent flat band networks, all one needs is to choose CLS sets which are linearly dependent, and then apply the above generator scheme for non-orthogonal flat bands. For 1D networks it was shown by Maimaiti et al. that a linearly dependent CLS set can be reduced to a set with smaller CLSs, and in the case of band touching a dispersive band or even crossing it to an orthonormal CLS set [16], [17]. In higher dimensions linearly dependent flat bands lead to band touching which can be separated additionally into linear touching (with two dispersive bands e.g. Figure 1), or quadratic touching (with only one dispersive band, e.g. Figures 3(c) and 7). Recent studies of Graf et al. [19] and Hwang et al. [20] use the transformation of CLSs into Bloch representation to formulate linear dependence conditions in reciprocal space and to come up with a final generator of linearly dependent flat band networks.

The above generators can also be extended to the case of non-Hermitian Hamiltonians with flat bands [58], relevant in photonics. Non-Hermitian flat bands keep some of the above listed properties of the Hermitian flat bands, e.g. formation of continuous manifolds, but further studies are required. Also a number of further more specialized flat band generators have been reported, among them the origami rules [59], repetitions of mini-arrays [60], Moiré engineering [61], local symmetry partitioning [62], and path-exchange [63].

We close this section with discussing the case of Wannier-Stark (WS) flat bands [64]. One starts with a tight binding network on a Bravais lattice in dimension $d \geq 2$, e.g. the simple 2D square lattice with nearest neighbour hopping. Its band structure consists out of one band with energy depending on the two components of the Bloch momentum vector. Next one applies a dc field along some direction, which induces onsite energies growing linearly along this field direction. We can consider the field direction as a tunable parameter. Translational invariance is broken along the field direction in general. However the translational

invariance perpendicular to the field direction can be preserved (or fine-tuned) for certain rational field directions – actually for an infinite amount of them. These cases lead to an infinite equidistant ladder of WS bands as functions of some perpendicular Bloch momentum vector of dimension $(d - 1)$. However each eigenstate is still d-dimensional, even though its amplitudes along the field direction decay super-exponentially in both directions. As shown by Mallick et al. in Ref. [64], almost all rational field directions (except for a few) will result in strictly flat WS bands, such that the WS band structure will consist of an infinite ladder of flat bands only. Transport is then completely suppressed. Yet the WS flat bands do not support CLSs, instead the wave function localizes at best superexponentially in all directions. This outcome is not in contradiction with above statements that ABF flat bands are orthonormal and support CLSs, since one condition for that is a finite number of bands. For WS flat bands the number of bands in the WS ladder is infinite instead. Finally we note that WS flat bands can be mapped onto Floquet systems in $d - 1$ dimensions.

4.2 Detuning

A flat band is fragile against perturbations, raising the question of how a flat band system responds to perturbations. Various types of perturbations of flat band Hamiltonians which can be experimentally implemented with photonics platforms have been considered over the years – e.g. dc fields, periodic driving, dissipative potentials. It emerged that, when properly arranged, these terms can result in unusual phases and phenomena. For instance, a properly tuned interplay between magnetic and two dc fields (perpendicular and longitudinal) yields Landau–Zener–Bloch oscillations in a 1D diamond chain [65], [68], as shown in Figure 9(a). Similarly, Bloch oscillations have been ignited in 1D Lieb lattices via non-hermitian driving [69]. Fine-tuned driving protocols of the hopping terms of flat band lattices can also result in displacing CLS throughout the network while retaining their spatial profile. This for instance resulted into the storage and transfer of CLS in the 2D Lieb [70] and non-abelian Thouless pumping of for instance CLS in a 1D stub-like chain [66] – with the latter one shown in Figure 9(b). Non-Hermitian [71], [72] and $\mathcal{PT}$-symmetric [73], [74] perturbations have been studied in flat band networks. In Ref. [67], exact CLS in $\mathcal{PT}$-symmetric sawtooth-like photonic flat band lattice have been theoretically predicted and experimentally verified (Figure 9(c)). It was also shown that properly tuned gain/loss terms can induce defect states [75] and stable laser emissions [76].

An important class of perturbations is *disorder*, where the response proved to be especially rich, depending both
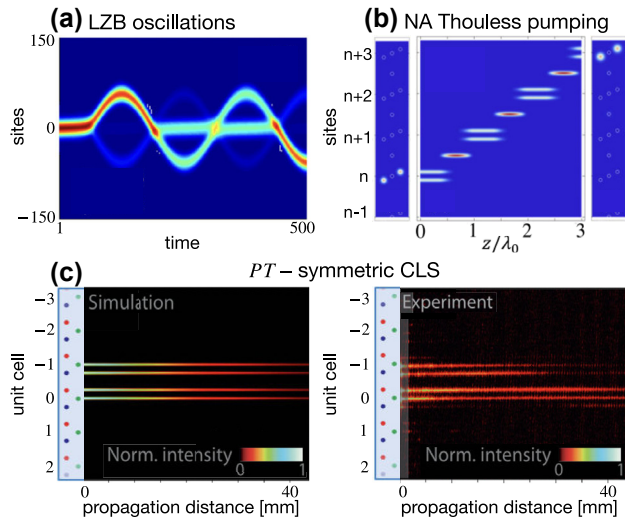
Figure 9: Examples of flat band detuning. (a) Landau–Zener–Bloch oscillations of an excited CLS in a diamond chain with non-zero perpendicular and longitudinal dc electric and magnetic fields. Reprinted with permission from Ref. [65]. (b) Non-abelian Thouless pumping of a CLS in a 1D stub-like chain via periodic modulation of the hopping terms of period $lambda_0$. Reprinted with permission from Ref. [66]. (c) Diffraction-free propagation of an excited CLS in a $\mathcal{PT}$-symmetric sawtooth-like photonic flat band lattice. The numerical simulation is shown in the left panel, and the experimental observation is shown in the right panel. Reprinted with permission from Ref. [67].

Figure 10: Fine-tuned metal-insulator transition disordered one-dimensional $\nu = 2$ flat band networks. (a) Cross-stitch lattice with anti-symmetric quasiperiodic perturbation of strength λ. The analytic mobility edge (black line) separates extended (blue) and localized (red) phases. Reprinted with permission from Ref. [77]. (b) Energy-resolved exponent average ratio of adjacent gaps $\langle r \rangle$ at weak disorder limit as a function of the ABF manifold angle θ. Reprinted with permission from Ref. [78].

networks lead to the emergence of critical phases and fractal edges separating critical and localised eigenstates in the spectrum, in analogy to mobility edges [92], [93]. The weak disorder results can be rationalised in the framework of projected models, where one considers a projection onto the flat band resulting in an effective single band model with finite and correlated disorder.

4.3 Applications in photonics

Optical waveguide arrays have formed a flexible platform for realizing many of the above fine-tuning effects. Waveguide arrays lend themselves naturally to implementation of flat bands thanks to the ability to precisely control the waveguide positions and thereby engineer the requisite fine-tuned coupling strengths and network geometries [94]. A variety of flat bands has been implemented in experiments using waveguide arrays including the sawtooth chain [41], stub chain [32], [95], diamond chain [31], [95], Sierpinsky gasket [33], [96], Lieb lattice [4]–[6], [27], [97], [98] (shown in Figure 11(a)), as well as lattices hosting line states [99] and nontrivial loop boundary states caused by band touchings [100]–[102].

Introducing a transverse or longitudinal modulation to the waveguides can be used to implement various driving perturbation terms to flat band lattices. For example, the flat band in the diamond chain has been shown to be robust in the presence of external driving along the lattice axis [103]. Fine-tuning of periodic longitudinal driving in square lattices can create Floquet flat bands with non-trivial topology [104]–[106], shown in Figure 11(b), and non-abelian Thouless pumping of spatially compact excitations [107]. Transverse driving has been used to observe Bloch oscillations in photonic rhombic lattices [108].

on the type of the flat band and the type of disorder. The impact of uncorrelated disorder has been broadly studied [63], [79]–[84]. In particular, the weak disorder regime demonstrated unconventional scaling of the localization length in 1D lattices hosting both orthogonal [15], [79] and non-orthogonal flat bands [80]. Anomalous scalings have been also observed in higher dimensional lattices – e.g. in 2D Lieb [82] as well as in 3D Lieb lattices [83], [84] due to uncorrelated disorder. The introduction of correlations, e.g. quasiperiodicity, can introduce mobility edges [77], [85] as shown in Figure 10(a). Correlations in the disorder might also induce the inverse Anderson transition [86], [87]. Flat bands with a band touching, non-orthonormal and incomplete set of CLS, can induce critical states at the FB energy in presence of the weak uncorrelated onsite disorder [43]. In some scenarios flat bands turned out to be immune to disorder due to a symmetry protection [28], [86]. All-bands-flat Hamiltonians are especially sensitive to different types of disorder [88]. In particular, they can exhibit a metal-insulator transition for weak/infinitesimal disorder driven by the position of the Hamiltonian on the ABF manifold [78] as illustrated in Figure 10(b). As a consequence, the ABF networks with a metallic phase at weak disorder undergo a re-entrant localization transition at finite disorder strengths [89]–[91]. Quasiperiodic perturbations of all-bands-flat
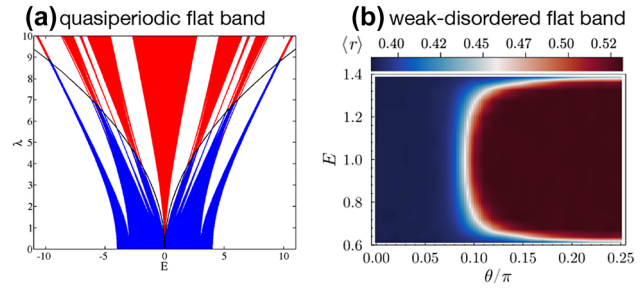
Typically in nanophotonic systems fine-tuning is an essential ingredient for the realization of flat bands, owing to the inevitable presence of long-range couplings that cannot be precisely controlled. For example, fine-tuning of the radius of dielectric rods in 2D photonic crystals was used to obtain an accidental degeneracy similar to the flat band of the Lieb lattice, first at microwave frequencies [110] and subsequently in optical metamaterials [111]. The emergence of flat bands in fine-tuned photonic crystals can be understood semi-analytically using perturbation theory in Fourier space by taking into account scattering between different wavevectors induced by the periodic refractive index modulation combined with symmetry-breaking perturbations [109], [112]. An example of a fine-tuned photonic crystal flat band is shown in Figure 11(c). Modifications to this perturbation theory [113]–[115] have enabled the description of flat bands in photonic moiré superlattices [23]–[26], [116], [117], shown in Figure 11(d), which are difficult to study using direct numerical simulations due to their large unit cell size.

Another inevitable ingredient of nanophotonic systems is losses – either through absorption or radiation to the far field, making this an ideal playground for exploring the physics of non-Hermitian flat bands. For example, the physics of non-Hermitian $\mathcal{PT}$-symmetric flat bands was explored using waveguide arrays with losses introduced by periodically inscribing strong scattering centres [67] (Figure 9(c)). In the case of passive photonic crystals, the light cone marks a transition between bound and lossy modes that must be taken into account when fine-tuning degeneracies in the band structure [118]. Mie theory provides a powerful semi-analytical approach for taking into account the interplay between local couplings and far-field radiation when engineering strong degeneracies of nanophotonic systems [119].

A recent experimental study on the border line between condensed matter and photonics – a Bose–Einstein condensate of ^{87}Rb atoms loaded into an optical momentum lattice supported by various laser beams – tested the impact of disorder on flat band states [120], [121]. The work reports on the realization of a sawtooth chain (coined Tasaki lattice in Ref. [120], [121]) and the observation of the transition from flat band localization (i.e. compact localized states) to Anderson localization similar to theoretical predictions discussed above.

The interested reader can find more details on photonic flat bands in the recent reviews [3], [122].
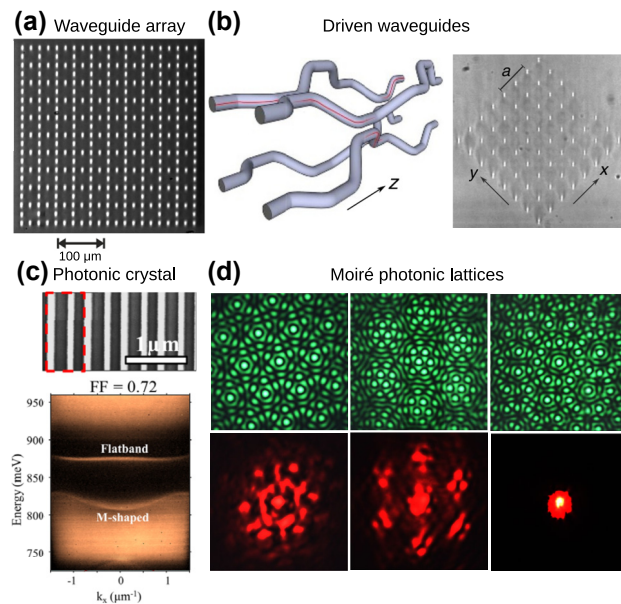
5 Interactions

Flat bands and compact localized eigenstates are linear (single particle) concepts. However, in photonics material-mediated photon–photon interactions naturally occur for strong optical power. For many photons in the classical regime mean-field nonlinear terms appear in the governing equations [123]. These nonlinear terms extend the dynamical regimes way beyond the Bloch band structure based one, allowing even for thermalization and chaos. Likewise in quantum interacting regimes, also accessible with photonic platforms [124], [125], in general single particle CLS are replaced by extended many-body states. The impact that photonic interactions may have on flat bands including the unconventional phenomena they may unlock depend on the chosen lattice. From a fine-tuning standpoint, this quest for unusual phases can be rephrased as (i) find sub-families of flat band networks for given interactions, or (ii) tune special interactions to yield certain phenomena upon sub-families of flat band networks.

5.1 Nonlinear regime

Destructive interference – the underlying principle behind the existence of CLS – is a concept which is not restricted

Figure 11: Examples of platforms for photonic flat bands.
(a) Laser-written waveguide array implementing the 2D Lieb lattice. Reprinted with permission from Ref. [97]. (b) Longitudinally-modulated waveguide array implementing a Floquet flat band. Reprinted with permission from Ref. [105]. (c) 1D photonic crystal exhibiting a flat band at a fine-tuned value of its filling factor (FF) and its angle-resolved reflectivity spectrum. Reprinted with permission from Ref. [109]. (d) Optically-induced moiré photonic lattices (top row) revealing twist angle-controlled localization of a probe beam (bottom row). Reprinted with permission from Ref. [23].

only to the linear regime of a lattice. Hence, the fine-tuning approach for generating lattices supporting CLS and their flat bands can be extended to generating nonlinear lattices which support strictly compact photonic excitations (as opposed to standard solitary excitations). Such compact solutions can be considered as extensions of linear CLS into the nonlinear regime, and they are special cases of a broad class of spatially localized time-periodic solutions of nonlinear lattices called *discrete breathers* [126]–[131]. These solutions – also known as *intrinsic localized modes* – have been studied in the realm of nonlinear optics [132] and they have been experimentally observed e.g. with waveguide arrays [133], [134] and optical fibers [135].

Strictly compact breathers harvesting on destructive interference have then been found in several flat band models in presence of Kerr nonlinearity in the past decade, from the Kagome to the diamond chain [136]–[141]. One of these sample cases is the nonlinear sawtooth chain [136] shown in Figure 12(a). This unfolded version of Figure 3(b) is an arrangement which facilitates the experimental realization by drastically reducing longer range hoppings [41]. The CLS profile is shown with blue and red dots. The amplitudes in the blue sites are rescaled by a prefactor α with respect to the amplitude in the red site, with α depending on the hopping strengths of the lattice. In presence of a Kerr nonlinearity, the compact breather (Figure 12(b)) continues to exist at a specific fine-tuned condition between the nonlinear strength and the hopping strengths. However, when this condition is slightly violated, the compact breather gains exponential tails and turns into a regular discrete breather (Figure 12(c)). In other words, compact breathers of the nonlinear sawtooth lattice in Figure 12(a) are special fine-tuned cases of continuous families of exponentially localized discrete breathers.
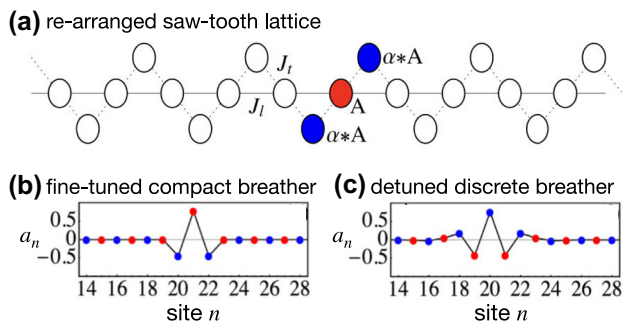
The compact breather fine-tuning for the sawtooth lattice is due to the linear CLS of the model having different amplitudes at different sites. At variance, the linear CLS of the cross-stitch lattice (Figure 3(a)) can be continued as a compact breather to any nonlinear strength. In this case, the Kerr term parametrically shifts the CLS frequency while keeping its spatial profile intact [141]. The reason is the homogeneity of the linear CLS. Indeed, in the cross-stitch all non-zero CLS components have same amplitude up to phase factors, while this condition in the CLS of the sawtooth is violated by the prefactor α. This fact has been formalized into a criterium stating that for Kerr nonlinearity any homogeneous CLS can be continued as compact breathers in the nonlinear regime, with the nonlinear strength parametrically shifting their frequency [141]. On the other hand, non-homogeneous CLS can be continued as discrete breathers in the nonlinear regime of a flat band lattice, and compactness can be accidentally re-obtained at fine-tuning conditions involving the nonlinear strength and hopping parameters.

Building upon these results and sample cases, the real space flat band generator [16]–[18] discussed in Sec. 4.1 has been adapted to the nonlinear case and turned into systematic compact breathers generator [142]. Such schemes do not assume the homogeneity condition of compact breathers or even the presence of any flat band in the linear system, and can be extended to considerations of fine-tuned non-local nonlinear terms [142]. Together with their existence criteria, it has been found that linear instability of compact breathers arises from resonance mechanism between the breather itself and linear oscillations of the underlying lattice [136], [141]. In short, their frequency should be tuned away from the dispersive part of the spectrum of the linear flat band system. This is visualized in Figure 13, where a slightly perturbed compact breather of the cross-stitch is tuned to two different frequencies via the nonlinear strength. A stable case where resonances are avoided
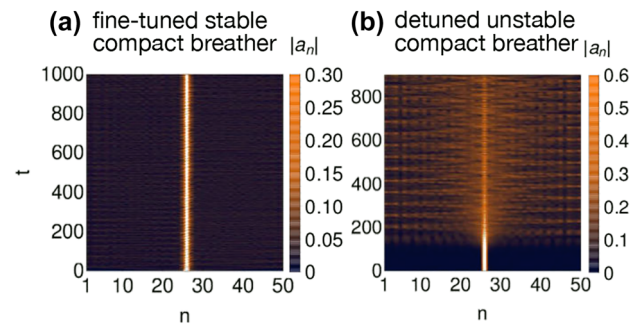

(a) re-arranged saw-tooth lattice

(b) fine-tuned compact breather **(c)** detuned discrete breather

Figure 12: Sawtooth lattice with Kerr nonlinearity. (a) Lattice profile. The CLS is colored in blue and red, where $\alpha = -J_l/J_t$. (b) Spatial profile of a compact breather fine-tuned at specific strengths of nonlinearity and hopping terms. (c) Spatial profile of a non-compact discrete breather at slightly detuned nonlinear and hopping strengths with respect to (b). Reprinted with permission from Ref. [136].

(a) fine-tuned stable compact breather $|a_n|$ **(b)** detuned unstable compact breather $|a_n|$

Figure 13: Stable (a) and unstable (b) propagation of an initially excited compact breather in a cross-stitch lattice with Kerr nonlinearity for two different nonlinear strengths. Reprinted with permission from Ref. [141].

is shown in Figure 13(a), while an unstable one is shown in Figure 13(b) where the breather frequency is tuned to resonate with linear dispersive modes.

The impact of compact breathers on the dynamics of nonlinear flat band networks is still a rather unexplored yet promising research area. For instance, it has been shown that compact breathers can turn into tunable nonlinear Fano resonances [143] for the propagation of light (a mechanism also ignited by onsite impurities in flat bands) [144]. It is also possible to use nonlinear flat bands with non-Hermitian impurities to engineer coherent perfect absorbers (also known time-reversed lasers) [72]. Furthermore, nonlinear flat band lattices can also allow control over the mobility of discrete solitons, as it has been demonstrated in the nonlinear Kagome [137] and nonlinear Lieb lattice [140].

All-band-flat networks demonstrate the highest sensitivity to nonlinearity. Since the linear part lacks any transport, nonlinear perturbations will in general restore transport. Surprisingly, in the nonlinear diamond chain with fine-tuned magnetic flux (Figure 5), any spatially compact initial excitation remains therein confined along the propagation. In other words, Kerr nonlinearity does not destroy linear caging for that system [145], [146]. Indeed, generic nonlinear interactions including Kerr nonlinearity upon the manifold of all-bands-flat networks destroy caging and induce transport [48]. Caging then is restored for fine-tuned families of ABF linear lattices. An example is shown in Figure 14(a) and (b) for two cases of the family of 1D two bands ABF networks with Kerr nonlinearity. A fine-tuned lattice in Figure 14(a) (which corresponds to the Creutz ladder [147]) retains strict nonlinear caging as an initially compact excitation remains

therein localized. On the other hand, in a detuned ABF lattice in Figure 14(b) the initially compact excitation is propagating into the chain, confirming that caging is lost. We also mention the impact of nonlinearity on momentum space linear Bloch modes which results in bifurcations and instabilities and the formation of localized states [148].

5.2 Quantum regime – a perspective

The quantized analog of the Kerr nonlinearity is the two-body interaction containing a product of two creation and two annihilation operators. Its impact has been intensively studied in recent years in flat band networks from a mathematical and applied condensed matter perspective. The challenge of making photons interact results in interaction induced via e.g. doped media [124], [125] or through the optical nonlinear terms at the level of individual photons [149]. Most studies focused on finite-particle density regimes (i.e. where the ratio between the number of particle and the lattice size is constant). This has been a prolific research direction, as over the years phenomena of condensation and superconductivity have been discovered [150]–[154], together with phenomena of absence of charge transport known as many-body flat band localization [155]–[157], disorder-free localization [158], [159], magnon crystallization [160]–[162] and quantum many-body scars [56], [163]–[167]. Some of these works harvested on the real space generator scheme for single particle lattices to highlight fine-tuned manifolds of interacting flat band networks exhibiting many-body flat band localization and quantum scars [56], [155], [159].

Since photons are bosons, they can occupy the same single particle state. As a rule of the thumb occupation numbers of five or more photons per single particle state reduce most of the physics back to the nonlinear description. Scaling down from the finite particle density regimes to fixed number of particles, higher dimensional linear photonic networks have been employed to study few quantum interacting particles in lattices. For instance, the dynamics of two interacting bosons in one-dimensional disordered chains has been probed via two-dimensional photonic lattices, where the Hubbard interaction turns into an onsite diagonal term [168] – an approach which has been tested experimentally [169] and also employed for three interacting bosons [170]. In the context of flat bands, this approach has been used to study the dynamics of two interacting bosons in 1D two band ABF networks with Bose–Hubbard interaction [56], shown in Figure 14(c) and (d). The propagation of two bosons initially located in the same unit-cell is obtained for the same two lattices used to visualize the nonlinear caging [fine-tuned network in Figure 14(a)] and its breaking
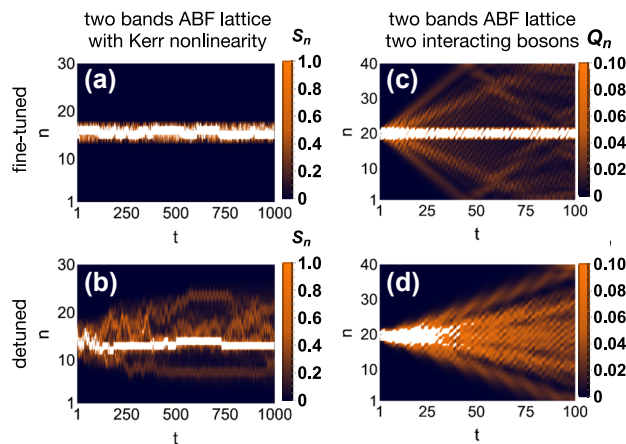

Figure 14: Interaction in $\nu = 2$ ABF lattices. (a–b) Time evolution of nonlinear spatially compact excitations for a fine-tuned (a) and non fine-tuned case (b). (c–d) Same as (a–b) for two interacting bosons. Reprinted with permission from Ref. [48], [56].

[detuned network in Figure 14(b)]. In both lattices, a part of the probability distribution propagates ballistically, indicating the spreading of the particle pair along the networks. However, in the fine-tuned case Figure 14(c), a substantial fraction of the probability distribution remains frozen around the unit cell where both particles were initially located. This frozen portion of the distribution is instead absent in the detuned case Figure 14(d). Such phenomenon is due to overlap between the initial condition and energy-renormalized two particles caged states, whose existence is ensured by the very same fine-tuning condition that guarantee nonlinear caging in the classical nonlinear regime [56]. These two-particles compact states in ABF network can be found also for larger finite number of particles, and they generalize the single particle CLS [56]. Furthermore, such many-body CLS can be fine-tuned in networks which host a mix of flat and dispersive bands [163]–[166], [171]. However, the challenge of turning them into "localized quantum states of light" in photonic lattices (as dubbed in Ref. [95]) remains to this date an exciting research direction. The utilization of quantum many-body physics of interacting photons [95], [124], [125], [149] for flat band networks is still an avenue to be explored.

5.3 Applications in photonics

Interactions in photonics usually appear in the form of mean-field nonlinearities, arising due to the Kerr effect or saturable gain. Thus, most experiments studying the interplay between interactions and flat bands have focused on this limit, with the aim of exploring novel paradigms for the design and control of lasers and other nonlinear optical devices.

Exciton–polariton condensates in structured microcavities are a particularly valuable platform, given that they support strong repulsive Kerr nonlinearity (inherited from their excitonic component) and fine-tuned gain and loss landscapes can be created by adjusting the spatial profile of the external pump laser [172]. For example, Baboux et al. [173] observed exciton–polariton condensation in a quasi-one-dimensional stub lattice of micropillars, finding that the flat band condensates become fragmented with a low coherence length due to the intrinsic fabrication disorder, preventing phase-locking between different compact localized states, as shown in Figure 15(a). These observations suggest a need to implement controlled perturbations (stronger than any underlying disorder) to observe flat band-derived condensates or lasing with non-trivial long-ranged correlations. A more recent study using the exciton-polariton platform has illustrated how the driven-dissipative dynamics of media with saturable gain can be surprisingly
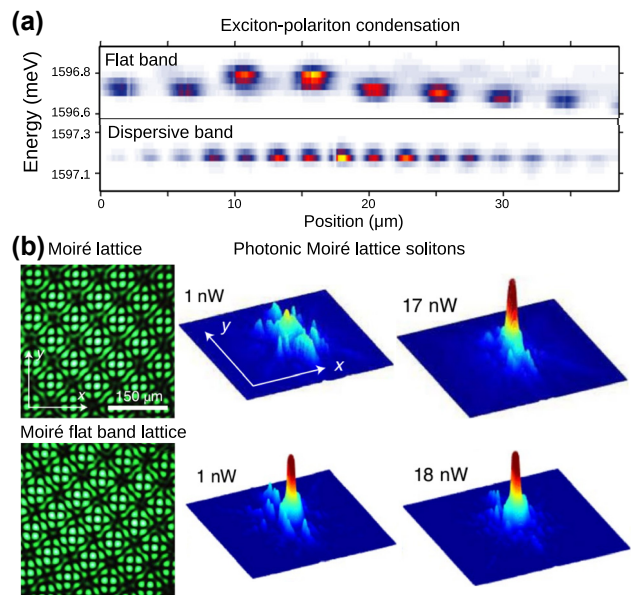

Figure 15: Photonics experiments combining flat bands with nonlinearity. (a) Spatially-resolved emission spectra from flat band and dispersive band exciton–polariton condensates, Reprinted with permission from Ref. [173]. The former exhibits fragmentation into many incoherent condensates due to disorder-induced condensates, while the lattice exhibits coherence over many lattice sites. (b) Soliton formation in a optically-induced photonic moiré lattices, Reprinted with permission from Ref. [178]. For a twist angle corresponding to a flat band, strong localization is observed for both low power (linear) and high power (nonlinear) probe beams. Tuning away from this critical twist angle yields strong diffraction in the linear limit.

counter-intuitive; novel classes of localized modes can be created by engineering of the pump spatial profile and phase [174] even when the underlying lattice does not host any flat bands.

Another experimental platform promising for the study of interactions in flat bands which has emerged in the last few years is nonlinear waveguide arrays. For example, even though the ambient Kerr nonlinearity of laser-written waveguide arrays is relatively weak, sufficiently high intensities leading to the formation of discrete solitons [175] can be achieved using pulsed lasers. Recent experiments have observed bulk and edge solitons in complex two-dimensional driven lattices [176], [177] that can be fine-tuned to obtain Floquet flat bands [104], [105].

One complication with studying interactions in the flat band limit using pulsed lasers is the finite bandwidth of the probe laser combined with the inevitable frequency dispersion of the coupling coefficients; even if one has fine-tuned the lattice parameters to obtain a flat band at the central frequency of the probe, the spatial dispersion for other frequencies will be nonzero, leading to diffraction and

making it difficult to unambiguously observe nonlinearity-induced delocalization of the flat band state. A potential solution to this problem is to use more sophisticated Floquet driving schemes to minimize the frequency dispersion of the coupling coefficients [179], in effect creating a flat band in the frequency domain [180].

Another alternative is to use optically-induced waveguides photorefractive materials, which support both fine-tuning and the ability to observe nonlinear effects using a continuous wave probe laser [101], which has enabled the recent observation of solitons in moiré superlattices [178], shown in Figure 15(b).

Turning to photonic crystals and metasurfaces, the integration of optical gain media into these structures is enabling the development of novel lasers based on concepts from topological photonics [181]–[185]. While these studies largely focus on designs insensitive to perturbations, owing to the presence of difficult-to-control long-range couplings, these structures can also support compact localized resonances and flat bands arising from the interplay between radiation losses and fine-tuning of the structural parameters [24], [119], [186]–[188]. Beyond lasing, flat bands in photonic crystals show promise as a means of enhancing light–matter interactions [189].

Photonic lattices can also be used to simulate different quantum systems, including interacting flat band models – known as *photonic quantum simulators* [190], either using networks of optical cavities with ultrastrong nonlinearities [124] or by mapping the system of interest into a higher dimensional non-interacting system. The latter has been proposed for the Creutz ladder with Hubbard-like interaction [35] and demonstrated experimentally for the one-dimensional Hubbard model [191], paving the way to probe many interesting phenomena related to the interplay of topology and interactions. Another useful technique in this direction is the ability to emulate high-dimensional lattices with tailored long-range interactions using time modulation and the concept of synthetic dimensions [192], enabling the recent emulation of a sawtooth flat band lattice using two coupled ring resonators [193].

A recent theoretical study showed that flat band induced trapping of excitations in a nonlinear ABF diamond chain is destroyed on the quantum level of two bosons and quickly recovered when increasing the bosonic occupation numbers [194]. In parallel Martinez et al. realized the setup using superconducting qubit arrays [195]. The experiments demonstrated that noninteracting photons are blocked due to the underlying ABF network, while the controlled adding of interaction lead to a transport of a pair of two interacting photons [195].

6 Summary and outlook

Flat bands provide a fascinating testbed for novel and interesting phases of matter that emerge in perturbed flat bands. The challenge is that flat bands require symmetries or fine-tuning to engineer them that often are far from obvious. One of the main results in the construction of flat bands is the not so obvious degree of flat band fine-tuning available. Despite flat bands systems being fine-tuned or protected by symmetry and therefore *a priori* fragile to perturbations, they form continuous manifolds in the space of Hamiltonian parameters, and many translationally invariant perturbations preserve the flatness. However, most physically relevant perturbations move the Hamiltonian away from that flat band manifold. Furthermore, perturbation can break the flatness of a band or allow for further fine-tuning allowing preserving the flatness, as happens with interactions where combining flat band lattices and interactions with the right degree of fine-tuning one can achieve nonergodic behaviour and suppress of some or all of the transport.

Flat bands react differently to perturbations allowing to engineer many interesting phenomena, including non-perturbative transitions. Orthogonal flat bands, e.g. with orthogonal CLS, are especially convenient for analysis. The effect of weak perturbations can be understood efficiently by projecting the perturbation onto the flat band resulting in an *effective* Hamiltonian. Orthogonality ensures that the projector onto the band is local, and therefore so is the effective projected model. These effective projected models can sometimes be mapped onto the known models, or provide helpful insights into the properties of the perturbed flat bands. Interactions further complicate the picture, however, further fine-tuning is possible which leads to emergent conservation laws that trap some particles, producing quantum caging, or suppress transport producing non-ergodic many-body systems.

Despite all the recent progress, we are confident that the best of flat band research still lies ahead of us, with numerous open questions to be addressed.

Author contributions: All authors have accepted responsibility for the entire content of this manuscript and approved its submission.

Conflict of interest: Authors state no conflicts of interest.

Informed consent: Informed consent was obtained from all individuals included in this study.

Ethical approval: The conducted research is not related to either human or animals use.

Data availability: Data sharing is not applicable to this article as no datasets were generated or analyzed during the current study.

References

[1] O. Derzhko, J. Richter, and M. Maksymenko, "Strongly correlated flat-band systems: the route from Heisenberg spins to Hubbard electrons," *Int. J. Mod. Phys. B*, vol. 29, no. 12, 2015, Art. no. 1530007.

[2] D. Leykam, A. Andreanov, and S. Flach, "Artificial flat band systems: from lattice models to experiments," *Adv. Phys.: X*, vol. 3, no. 1, 2018, Art. no. 1473052.

[3] D. Leykam and S. Flach, "Perspective: photonic flatbands," *APL Photonics*, vol. 3, no. 7, 2018, Art. no. 070901.

[4] R. A. Vicencio, *et al*., "Observation of localized states in Lieb photonic lattices," *Phys. Rev. Lett.*, vol. 114, no. 24, 2015, Art. no. 245503.

[5] S. Mukherjee, *et al*., "Observation of a localized flat-band state in a photonic Lieb lattice," *Phys. Rev. Lett.*, vol. 114, no. 24, 2015, Art. no. 245504.

[6] S. Xia, Y. Hu, D. Song, Y. Zong, L. Tang, and Z. Chen, "Demonstration of flat-band image transmission in optically induced Lieb photonic lattices," *Opt. Lett.*, vol. 41, no. 7, pp. 1435−1438, 2016.

[7] M. Kohmoto and B. Sutherland, "Electronic states on a penrose lattice," *Phys. Rev. Lett.*, vol. 56, no. 25, pp. 2740−2743, 1986.

[8] B. Sutherland, "Localization of electronic wave functions due to local topology," *Phys. Rev. B*, vol. 34, no. 8, pp. 5208−5211, 1986.

[9] E. H. Lieb, "Two theorems on the Hubbard model," *Phys. Rev. Lett.*, vol. 62, no. 10, pp. 1201−1204, 1989.

[10] A. Mielke, "Ferromagnetism in the Hubbard model on line graphs and further considerations," *J. Phys. A: Math. Gen.*, vol. 24, no. 14, p. 3311, 1991.

[11] H. Tasaki, "Ferromagnetism in the Hubbard models with degenerate single-electron ground states," *Phys. Rev. Lett.*, vol. 69, no. 10, pp. 1608−1611, 1992.

[12] G. Tarnopolsky, A. J. Kruchkov, and A. Vishwanath, "Origin of magic angles in twisted bilayer graphene," *Phys. Rev. Lett.*, vol. 122, no. 10, 2019, Art. no. 106405.

[13] H. Ha and B.-J. Yang, "Macroscopically degenerate localized zero-energy states of quasicrystalline bilayer systems in the strong coupling limit," *Phys. Rev. B*, vol. 104, no. 16, 2021, Art. no. 165112.

[14] Y. Huang, X. Li, H. Cui, and Z. Zhou, "Bi-layer graphene: structure, properties, preparation and prospects," *Curr. Graphene Sci.*, vol. 2, no. 2, pp. 97−105, 2019.

[15] S. Flach, D. Leykam, J. D. Bodyfelt, P. Matthies, and A. S. Desyatnikov, "Detangling flat bands into Fano lattices," *Europhys. Lett.*, vol. 105, no. 3, 2014, Art. no. 30001.

[16] W. Maimaiti, A. Andreanov, H. C. Park, O. Gendelman, and S. Flach, "Compact localized states and flat-band generators in one dimension," *Phys. Rev. B*, vol. 95, no. 11, 2017, Art. no. 115135.

[17] W. Maimaiti, S. Flach, and A. Andreanov, "Universal $d = 1$ flat band generator from compact localized states," *Phys. Rev. B*, vol. 99, no. 12, 2019, Art. no. 125129.

[18] W. Maimaiti, A. Andreanov, and S. Flach, "Flat-band generator in two dimensions," *Phys. Rev. B*, vol. 103, no. 16, 2021, Art. no. 165116.

[19] A. Graf and F. Piéchon, "Designing flat-band tight-binding models with tunable multifold band touching points," *Phys. Rev. B*, vol. 104, no. 19, 2021, Art. no. 195128.

[20] Y. Hwang, J.-W. Rhim, and B.-J. Yang, "General construction of flat bands with and without band crossings based on wave function singularity," *Phys. Rev. B*, vol. 104, no. 8, 2021, Art. no. 085144.

[21] M. R. Slot, *et al*., "Experimental realization and characterization of an electronic Lieb lattice," *Nat. Phys.*, vol. 13, no. 7, pp. 672−676, 2017.

[22] R. Drost, T. Ojanen, A. Harju, and P. Liljeroth, "Topological states in engineered atomic lattices," *Nat. Phys.*, vol. 13, no. 7, pp. 668−671, 2017.

[23] P. Wang, *et al*., "Localization and delocalization of light in photonic moiré lattices," *Nature*, vol. 577, no. 7788, pp. 42−46, 2020.

[24] X.-R. Mao, Z. K. Shao, H. Y. Luan, and S. L. Wang, "Magic-angle lasers in nanostructured moiré superlattice," *Nat. Nanotechnol.*, vol. 16, no. 10, pp. 1099−1105, 2021.

[25] D. X. Nguyen, X. Letartre, E. Drouard, P. Viktorovitch, H. C. Nguyen, and H. S. Nguyen, "Magic configurations in moiré superlattice of bilayer photonic crystals: almost-perfect flatbands and unconventional localization," *Phys. Rev. Res.*, vol. 4, no. 3, p. L032031, 2022.

[26] L. Du, M. R. Molas, Z. Huang, G. Zhang, F. Wang, and Z. Sun, "Moiré photonics and optoelectronics," *Science*, vol. 379, no. 6639, 2023, Art. no. eadg0014.

[27] D. Roman-Cortes, G. Fadic, C. Cid-Lara, D. Guzmán-Silva, B. Real, and R. A. Vicencio, "Strain induced localization to delocalization transition on a Lieb photonic ribbon lattice," *Sci. Rep.*, vol. 11, no. 1, 2021, Art. no. 21411.

[28] A. Ramachandran, A. Andreanov, and S. Flach, "Chiral flat bands: existence, engineering, and stability," *Phys. Rev. B*, vol. 96, no. 16, p. 161104(R), 2017.

[29] A. Mallick, N. Chang, A. Andreanov, and S. Flach, "Anti-$\mathcal{PT}$ flatbands," *Phys. Rev. A*, vol. 105, no. 2, p. L021305, 2022.

[30] D. Calugaru, *et al*., "General construction and topological classification of crystalline flat bands," *Nat. Phys.*, vol. 18, no. 2, pp. 185−189, 2022.

[31] S. Mukherjee and R. R. Thomson, "Observation of localized flat-band modes in a quasi-one-dimensional photonic rhombic lattice," *Opt. Lett.*, vol. 40, no. 23, pp. 5443−5446, 2015.

[32] B. Real, *et al*., "Flat-band light dynamics in Stub photonic lattices," *Sci. Rep.*, vol. 7, no. 1, 2017, Art. no. 15085.

[33] H. Hanafi, P. Menz, A. McWilliam, J. Imbrock, and C. Denz, "Localized dynamics arising from multiple flat bands in a decorated photonic Lieb lattice," *APL Photonics*, vol. 7, no. 11, 2022, Art. no. 111301.

[34] N. Read, "Compactly supported Wannier functions and algebraic *K*-theory," *Phys. Rev. B*, vol. 95, no. 11, 2017, Art. no. 115309.

[35] J. Zurita, C. E. Creffield, and G. Platero, "Topology and interactions in the photonic Creutz and creutz-hubbard ladders," *Adv. Quantum Technol.*, vol. 3, no. 2, 2020, Art. no. 1900105.

[36] J. S. C. Hung, *et al*., "Quantum simulation of the bosonic Creutz ladder with a parametric cavity," *Phys. Rev. Lett.*, vol. 127, no. 10, 2021, Art. no. 100503.

[37] H. K. Jin, J. H. Han, and Y. Shin, "Creutz ladder in a resonantly shaken 1D optical lattice," *New J. Phys.*, vol. 22, no. 1, 2020, Art. no. 013023.

[38] P. Sathe, F. Harper, and R. Roy, "Compactly supported Wannier functions and strictly local projectors," *J. Phys. A: Math. Theor.*, vol. 54, no. 33, 2021, Art. no. 335302.

[39] P. Sathe and R. Roy, "Compact Wannier functions in one dimension," *Phys. Rev. B*, vol. 109 no. 15, 2024, Art. no. 155150.

[40] S. D. Huber and E. Altman, "Bose condensation in flat bands," *Phys. Rev. B*, vol. 82, no. 18, 2010, Art. no. 184502.

[41] S. Weimann, L. Morales-Inostroza, B. Real, C. Cantillano, A. Szameit, and R. A. Vicencio, "Transport in Sawtooth photonic lattices," *Opt. Lett.*, vol. 41, no. 11, pp. 2414−2417, 2016.

[42] Y. Zong, *et al*., "Observation of localized flat-band states in Kagome photonic lattices," *Opt. Express*, vol. 24, no. 8, pp. 8877−8885, 2016.

[43] J. T. Chalker, T. S. Pickles, and P. Shukla, "Anderson localization in tight-binding models with flat bands," *Phys. Rev. B*, vol. 82, no. 10, 2010, Art. no. 104209.

[44] H. Yan, *et al*., "Classification of classical spin liquids: typology and resulting landscape," 2023, arXiv: 2305.00155 [cond-mat.str-el].

[45] H. Yan, *et al*., "Classification of classical spin liquids: detailed formalism and suite of examples," 2023, arXiv: 2305.19189 [cond-mat.str-el].

[46] J.-W. Rhim and B.-J. Yang, "Classification of flat bands according to the band-crossing singularity of Bloch wave functions," *Phys. Rev. B*, vol. 99, no. 4, 2019, Art. no. 045107.

[47] J.-W. Rhim and B.-J. Yang, "Singular flat bands," *Adv. Phys.: X*, vol. 6, no. 1, 2021, Art. no. 1901606.

[48] C. Danieli, A. Andreanov, T. Mithun, and S. Flach, "Nonlinear caging in all-bands-flat lattices," *Phys. Rev. B*, vol. 104, no. 8, 2021, Art. no. 085131.

[49] P. Sathe and R. Roy, "Topological triviality of flat Hamiltonians," 2023, arXiv: 2309.06487 [cond-mat.mes-hall].

[50] J. Vidal, R. Mosseri, and B. Doucot, "Aharonov-bohm cages in two-dimensional structures," *Phys. Rev. Lett.*, vol. 81, no. 26, pp. 5888−5891, 1998.

[51] J. Vidal, B. Douçot, R. Mosseri, and P. Butaud, "Interaction induced delocalization for two particles in a periodic potential," *Phys. Rev. Lett.*, vol. 85, no. 18, pp. 3906−3909, 2000.

[52] S. Mukherjee, M. Di Liberto, P. Öhberg, R. R. Thomson, and N. Goldman, "Experimental observation of aharonov-bohm cages in photonic lattices," *Phys. Rev. Lett.*, vol. 121, no. 7, 2018, Art. no. 075502.

[53] M. Kremer, I. Petrides, E. Meyer, M. Heinrich, O. Zilberberg, and A. Szameit, "A square-root topological insulator with non-quantized indices realized with photonic Aharonov-Bohm cages," *Nat. Commun.*, vol. 11, no. 1, p. 907, 2020.

[54] C. Jörg, *et al*., "Artificial gauge field switching using orbital angular momentum modes in optical waveguides," *Light: Sci. Appl.*, vol. 9, no. 1, pp. 2047−7538, 2020.

[55] G. Cáceres-Aravena, D. Guzmán-Silva, I. Salinas, and R. A. Vicencio, "Controlled transport based on multiorbital aharonov-bohm photonic caging," *Phys. Rev. Lett.*, vol. 128, no. 25, 2022, Art. no. 256602.

[56] C. Danieli, A. Andreanov, T. Mithun, and S. Flach, "Quantum caging in interacting many-body all-bands-flat lattices," *Phys. Rev. B*, vol. 104, no. 8, 2021, Art. no. 085132.

[57] V. Brosco, L. Pilozzi, and C. Conti, "Two-flux tunable Aharonov-Bohm effect in a photonic lattice," *Phys. Rev. B*, vol. 104, no. 2, 2021, Art. no. 024306.

[58] W. Maimaiti and A. Andreanov, "Non-Hermitian flat-band generator in one dimension," *Phys. Rev. B*, vol. 104, no. 3, 2021, Art. no. 035115.

[59] R. G. Dias and J. D. Gouveia, "Origami rules for the construction of localized eigenstates of the Hubbard model in decorated lattices," *Sci. Rep.*, vol. 5, no. 1, 2015, Art. no. 16852.

[60] L. Morales-Inostroza and R. A. Vicencio, "Simple method to construct flat-band lattices," *Phys. Rev. A*, vol. 94, no. 4, 2016, Art. no. 043831.

[61] X. Zhou, *et al*., "Generation of isolated flat bands with tunable numbers through Moiré engineering," 2023, arXiv: 2310.07647 [cond-mat.mes-hall].

[62] M. Röntgen, C. V. Morfonios, and P. Schmelcher, "Compact localized states and flat bands from local symmetry partitioning," *Phys. Rev. B*, vol. 97, no. 3, 2018, Art. no. 035161.

[63] J.-H. Bae, T. Sedrakyan, and S. Maiti, "Isolated flat bands in 2D lattices based on a novel path-exchange symmetry," *SciPost Phys.*, vol. 15, p. 139, 2023.

[64] A. Mallick, N. Chang, W. Maimaiti, S. Flach, and A. Andreanov, "Wannier-Stark flatbands in Bravais lattices," *Phys. Rev. Res.*, vol. 3, no. 1, 2021, Art. no. 013174.

[65] R. Khomeriki and S. Flach, "Landau-zener Bloch oscillations with perturbed flat bands," *Phys. Rev. Lett.*, vol. 116, no. 24, 2016, Art. no. 245301.

[66] V. Brosco, L. Pilozzi, R. Fazio, and C. Conti, "Non-Abelian Thouless pumping in a photonic lattice," *Phys. Rev. A*, vol. 103, no. 6, 2021, Art. no. 063518.

[67] T. Biesenthal, M. Kremer, M. Heinrich, and A. Szameit, "Experimental realization of $\mathcal{PT}$-symmetric flat bands," *Phys. Rev. Lett.*, vol. 123, no. 18, 2019, Art. no. 183601.

[68] S. Xia, *et al*., "Band evolution and Landau-Zener Bloch oscillations in strained photonic rhombic lattices," *Opt. Express*, vol. 29, no. 23, pp. 37503−37514, 2021.

[69] S. Xia, *et al*., "Higher-order exceptional point and Landau-Zener Bloch oscillations in driven non-Hermitian photonic Lieb lattices," *APL Photonics*, vol. 6, no. 12, 2021, Art. no. 126106.

[70] M. Röntgen, C. Morfonios, I. Brouzos, F. Diakonos, and P. Schmelcher, "Quantum network transfer and storage with compact localized states induced by local symmetries," *Phys. Rev. Lett.*, vol. 123, no. 8, 2019, Art. no. 080504.

[71] D. Leykam, S. Flach, and Y. D. Chong, "Flat bands in lattices with non-Hermitian coupling," *Phys. Rev. B*, vol. 96, no. 6, 2017, Art. no. 064305.

[72] C. Danieli and T. Mithun, "Casting dissipative compact states in coherent perfect absorbers," *Phys. Rev. Res.*, vol. 2, no. 1, 2020, Art. no. 013054.

[73] Ge. Li, "Parity-time symmetry in a flat-band system," *Phys. Rev. A*, vol. 92, no. 5, 2015, Art. no. 052103.

[74] M. I. Molina, "Flat bands and PT-symmetry in quasi-one-dimensional lattices," *Phys. Rev. A*, vol. 92, p. 063813, 2015.

[75] B. Qi, L. Zhang, and L. Ge, "Defect states emerging from a non-hermitian flatband of photonic zero modes," *Phys. Rev. Lett.*, vol. 120, no. 9, 2018, Art. no. 093901.

[76] S. Longhi, "Photonic flat-band laser," *Opt. Lett.*, vol. 44, no. 2, pp. 287−290, 2019.

[77] J. D. Bodyfelt, D. Leykam, C. Danieli, X. Yu, and S. Flach, "Flatbands under correlated perturbations," *Phys. Rev. Lett.*, vol. 113, no. 23, 2014, Art. no. 236403.

[78] T. Cadez, Y. Kim, A. Andreanov, and S. Flach, "Metal-insulator transition in infinitesimally weakly disordered flat bands," *Phys. Rev. B*, vol. 104, no. 18, p. L180201, 2021.

[79] D. Leykam, S. Flach, O. Bahat-Treidel, and A. S. Desyatnikov, "Flat band states: disorder and nonlinearity," *Phys. Rev. B*, vol. 88, no. 22, 2013, Art. no. 224203.

[80] D. Leykam, J. D. Bodyfelt, A. S. Desyatnikov, and S. Flach, "Localization of weakly disordered flat band states," *Eur. Phys. J. B*, vol. 90, no. 1, p. 1, 2017.

[81] T. Bilitewski and R. Moessner, "Disordered flat bands on the kagome lattice," *Phys. Rev. B*, vol. 98, no. 23, 2018, Art. no. 235109.

[82] X. Mao, J. Liu, J. Zhong, and R. A. Römer, "Disorder effects in the two-dimensional Lieb lattice and its extensions," *Phys. E*, vol. 124, 2020, Art. no. 114340.

[83] J. Liu, X. Mao, J. Zhong, and R. A. Römer, "Localization, phases, and transitions in three-dimensional extended Lieb lattices," *Phys. Rev. B*, vol. 102, no. 17, 2020, Art. no. 174207.

[84] J. Liu, X. Mao, J. Zhong, and R. A. Römer, "Localization properties in Lieb lattices and their extensions," *Ann. Phys.*, vol. 435, 2021, Art. no. 168544.

[85] C. Danieli, J. D. Bodyfelt, and S. Flach, "Flat-band engineering of mobility edges," *Phys. Rev. B*, vol. 91, no. 23, 2015, Art. no. 235134.

[86] J. Liu, C. Danieli, J. Zhong, and R. A. Römer, "Unconventional delocalization in a family of three-dimensional Lieb lattices," *Phys. Rev. B*, vol. 106, no. 21, 2022, Art. no. 214204.

[87] C. Danieli, J. Liu, and R. A. Römer, "Quantum engineering for compactly localized states in disordered Lieb lattices," 2023, *arXiv:2309.04227*.

[88] G. Gligoric, D. Leykam, and A. Maluckov, "Influence of different disorder types on Aharonov-Bohm caging in the diamond chain," *Phys. Rev. A*, vol. 101, no. 2, 2020, Art. no. 023839.

[89] M. Goda, S. Nishino, and H. Matsuda, "Inverse Anderson transition caused by flatbands," *Phys. Rev. Lett.*, vol. 96, no. 12, 2006, Art. no. 126401.

[90] S. Longhi, "Inverse Anderson transition in photonic cages," *Opt. Lett.*, vol. 46, no. 12, p. 2872, 2021.

[91] H. Li, Z. Dong, S. Longhi, Q. Liang, D. Xie, and B. Yan, "Aharonov-bohm caging and inverse Anderson transition in ultracold atoms," *Phys. Rev. Lett.*, vol. 129, no.22, 2022, Art. no. 220403.

[92] S. Lee, A. Andreanov, and S. Flach, "Critical-to-insulator transitions and fractality edges in perturbed flat bands," *Phys. Rev. B*, vol. 107, 2023, Art. no. 014204.

[93] A. Aamna, A. Ramachandran, I. M. Khaymovich, and A. Sharma, "Flat band based multifractality in the all-band-flat diamond chain," *Phys. Rev. B*, vol. 106, no. 20, 2022, Art. no. 205119.

[94] J. Li, T. P. White, L. O'Faolain, A. Gomez-Iglesias, and T. F. Krauss, "Systematic design of flat band slow light in photonic crystal waveguides," *Opt. Express*, vol. 16, no. 9, pp. 6227−6232, 2008.

[95] S. Rojas-Rojas, L. Morales-Inostroza, R. A. Vicencio, and A. Delgado, "Quantum localized states in photonic flat-band lattices," *Phys. Rev. A*, vol. 96, no. 4, 2017, Art. no. 043803.

[96] E. Travkin, F. Diebel, and C. Denz, "Compact flat band states in optically induced flatland photonic lattices," *Appl. Phys. Lett.*, vol. 111, no. 1, 2017, Art. no. 011104.

[97] D. Guzmán-Silva, *et al*., "Experimental observation of bulk and edge transport in photonic Lieb lattices," *New J. Phys.*, vol. 16, no. 6, 2014, Art. no. 063061.

[98] D. Yu, L. Yuan, and X. Chen, "Isolated photonic flatband with the effective magnetic flux in a synthetic space including the frequency dimension," *Laser Photonics Rev.*, vol. 14, no. 11, 2020, Art. no. 2000041.

[99] S. Xia, *et al*., "Unconventional flatband line states in photonic Lieb lattices," *Phys. Rev. Lett.*, vol. 121, no. 26, 2018, Art. no. 263902.

[100] J. Ma, *et al*., "Direct observation of flatband loop states arising from nontrivial real-space topology," *Phys. Rev. Lett.*, vol. 124, no. 18, 2020, Art. no. 183901.

[101] L. Tang, *et al*., "Photonic flat-band lattices and unconventional light localization," *Nanophotonics*, vol. 9, no. 5, pp. 1161−1176, 2020.

[102] S. Gao, *et al*., "Demonstration of robust boundary modes in photonic decorated honeycomb lattices," *Adv. Opt. Mater.*, vol. 11, no. 2, 2022, Art. no. 2202045.

[103] S. Mukherjee and R. R. Thomson, "Observation of robust flat-band localization in driven photonic rhombic lattices," *Opt. Lett.*, vol. 42, no. 12, pp. 2243−2246, 2017.

[104] L. J. Maczewsky, J. M. Zeuner, S. Nolte, and A. Szameit, "Observation of photonic anomalous Floquet topological insulators," *Nat. Commun.*, vol. 8, no. 1, 2017, Art. no. 13756.

[105] S. Mukherjee, *et al*., "Experimental observation of anomalous topological edge modes in a slowly driven photonic lattice," *Nat. Commun.*, vol. 8, no. 1, 2017, Art. no. 13918.

[106] S. Afzal, T. J. Zimmerling, Y. Ren, D. Perron, and V. Van, "Realization of anomalous Floquet insulators in strongly coupled nanophotonic lattices," *Phys. Rev. Lett.*, vol. 124, no. 25, 2020, Art. no. 253601.

[107] Y.-Ke Sun, X. L. Zhang, F. Yu, Z. N. Tian, Q. D. Chen, and H. B. Sun, "Non-Abelian Thouless pumping in photonic waveguides," *Nat. Phys.*, vol. 18, no. 9, pp. 1080−1085, 2022.

[108] S. Xia, *et al*., "Observation of quincunx-shaped and dipole-like flatband states in photonic rhombic lattices without band-touching," *APL Photonics*, vol. 5, no. 1, 2020, Art. no. 016107.

[109] H. S. Nguyen, *et al*., "Symmetry breaking in photonic crystals: on-demand dispersion from flatband to Dirac cones," *Phys. Rev. Lett.*, vol. 120, no. 6, 2018, Art. no. 066102.

[110] X. Huang, Y. Lai, Z. H. Hang, H. Zheng, and C. T. Chan, "Dirac cones induced by accidental degeneracy in photonic crystals and zero-refractive-index materials," *Nat. Mater.*, vol. 10, no. 8, pp. 582−586, 2011.

[111] P. Moitra, Y. Yang, Z. Anderson, I. I. Kravchenko, D. P. Briggs, and J. Valentine, "Realization of an all-dielectric zero-index optical metamaterial," *Nat. Photonics*, vol. 7, no. 10, pp. 791−795, 2013.

[112] C. Munley, *et al*., "Visible wavelength flatband in a gallium phosphide metasurface," *ACS Photonics*, vol. 10, no. 8, pp. 2456−2460, 2023.

[113] B. Lou, N. Zhao, M. Minkov, C. Guo, M. Orenstein, and S. Fan, "Theory for twisted bilayer photonic crystal slabs," *Phys. Rev. Lett.*, vol. 126, no. 13, 2021, Art. no. 136101.

[114] K. Dong, *et al*., "Flat bands in magic-angle bilayer photonic crystals at small twists," *Phys. Rev. Lett.*, vol. 126, no. 22, 2021, Art. no. 223601.

[115] H. Tang, F. Du, S. Carr, C. DeVault, O. Mello, and E. Mazur, "Modeling the optical properties of twisted bilayer photonic crystals," *Light: Sci. Appl.*, vol. 10, no. 1, p. 157, 2021.

[116] S. S. Sunku, *et al*., "Photonic crystals for nano-light in moiré graphene superlattices," *Science*, vol. 362, no. 6419, pp. 1153−1156, 2018.

[117] C.-H. Yi, H. C. Park, and M. J. Park, "Strong interlayer coupling and stable topological flat bands in twisted bilayer photonic Moiré superlattices," *Light: Sci. Appl.*, vol. 11, no. 1, p. 289, 2022.

[118] X. Letartre, S. Mazauric, S. Cueff, T. Benyattou, H. S. Nguyen, and P. Viktorovitch, "Analytical non-Hermitian description of photonic crystals with arbitrary lateral and transverse symmetry," *Phys. Rev. A*, vol. 106, no. 3, 2022, Art. no. 033510.

[119] T. X. Hoang, H. S. Chu, F. J. García-Vidal, and C. E. Png, "High-performance dielectric nano-cavities for near- and mid-infrared frequency applications," *J. Opt.*, vol. 24, no. 9, 2022, Art. no. 094006.

[120] C. Zeng, *et al*., "Transition from flat-band localization to Anderson localization in a one-dimensional Tasaki lattice," *Phys. Rev. Lett.*, vol. 132, no. 6, 2024, Art. no. 063401.

[121] Y.-Yi Mao, *et al*., "Transition from flat-band localization to Anderson localization: realization and characterization in a one-dimensional momentum lattice," *Phys. Rev. A*, vol. 109, no. 2, 2024, Art. no. 023304.

[122] A. V. RodrigoPoblete, "Photonic flat band dynamics," *Adv. Phys.: X*, vol. 6, no. 1, 2021, Art. no. 1878057.

[123] Y. S. Kivshar and G. Agrawal, *Optical Solitons: From Fibers to Photonic Crystals*, San Diego, Academic Press, 2003.

[124] M. J. Hartmann, "Quantum simulation with interacting photons," *J. Opt.*, vol. 18, no. 10, 2016, Art. no. 104005.

[125] C. Noh and D. G. Angelakis, "Quantum simulations and many-body physics with light," *Rep. Prog. Phys.*, vol. 80, no. 1, 2016, Art. no. 016401.

[126] A. A. Ovchinnikov, "Localized long-lived vibrational states in molecular crystals," *JETP*, vol. 30, no. 1, p. 147, 1970.

[127] A. J. Sievers and S. Takeno, "Intrinsic localized modes in anharmonic crystals," *Phys. Rev. Lett.*, vol. 61, no. 8, pp. 970−973, 1988.

[128] R. S. MacKay and S. Aubry, "Proof of existence of breathers for time-reversible or Hamiltonian networks of weakly coupled oscillators," *Nonlinearity*, vol. 7, no. 6, p. 1623, 1994.

[129] S. Flach and C. R. Willis, "Discrete breathers," *Phys. Rep.*, vol. 295, no. 5, pp. 181−264, 1998.

[130] D. K. Campbell, S. Flach, and Y. S. Kivshar, "Localizing energy through nonlinearity and discreteness," *Phys. Today*, vol. 57, no. 1, pp. 43−49, 2004.

[131] S. Flach and A. V. Gorbach, "Discrete breathers - advances in theory and applications," *Phys. Rep.*, vol. 467, no. 1, pp. 1−116, 2008.

[132] F. Lederer, G. I. Stegeman, D. N. Christodoulides, G. Assanto, M. Segev, and Y. Silberberg, "Discrete solitons in optics," *Phys. Rep.*, vol. 463, no. 1, pp. 1−126, 2008.

[133] H. S. Eisenberg, Y. Silberberg, R. Morandotti, A. R. Boyd, and J. S. Aitchison, "Discrete spatial optical solitons in waveguide arrays," *Phys. Rev. Lett.*, vol. 81, no. 16, pp. 3383−3386, 1998.

[134] J. W. Fleischer, T. Carmon, M. Segev, N. K. Efremidis, and D. N. Christodoulides, "Observation of discrete solitons in optically induced real time waveguide arrays," *Phys. Rev. Lett.*, vol. 90, no. 2, 2003, Art. no. 023902.

[135] D. R. Solli, C. Ropers, P. Koonath, and B. Jalali, "Optical rogue waves," *Nature*, vol. 450, no. 7172, p. 1054, 2007.

[136] M. Johansson, U. Naether, and R. A. Vicencio, "Compactification tuning for nonlinear localized modes in sawtooth lattices," *Phys. Rev. E*, vol. 92, no. 3, 2015, Art. no. 032912.

[137] R. A. Vicencio, and M. Johansson, "Discrete flat-band solitons in the kagome lattice," *Phys. Rev. A*, vol. 87, no. 6, 2013, Art. no. 061803.

[138] G. Gligoric, A. Maluckov, L. Hadžievski, S. Flach, and B. A. Malomed, "Nonlinear localized flat-band modes with spin-orbit coupling," *Phys. Rev. B*, vol. 94, no. 14, 2016, Art. no. 144302.

[139] P. P. Belicev, G. Gligorić, A. Maluckov, M. Stepić, and M. Johansson, "Localized gap modes in nonlinear dimerized Lieb lattices," *Phys. Rev. A*, vol. 96, no. 6, 2017, Art. no. 063838.

[140] B. Real and R. A. Vicencio, "Controlled mobility of compact discrete solitons in nonlinear Lieb photonic lattices," *Phys. Rev. A*, vol. 98, no. 5, 2018, Art. no. 053845.

[141] C. Danieli, A. Maluckov, and S. Flach, "Compact discrete breathers on flat-band networks," *Low Temp. Phys.*, vol. 44, no. 7, pp. 678−687, 2018.

[142] D. Carlo and A. Andreanov, "Compact breathers generator in one-dimensional nonlinear networks," 2021, arXiv: 2104.11458 [nlin.PS].

[143] A. E. Miroshnichenko, S. Flach, and Y. S. Kivshar, "Fano resonances in nanoscale structures," *Rev. Mod. Phys.*, vol. 82, no. 3, pp. 2257−2298, 2010.

[144] A. Ramachandran, C. Danieli, and S. Flach, "Fano resonances in flat band networks," in *Fano Resonances in Optics and Microwaves: Physics and Applications*, E. Kamenetskii, A. Sadreev, and A. Miroshnichenko, Eds., Cham, Springer International Publishing, 2018, pp. 311−329.

[145] G. Gligoric, P. P. Beličev, D. Leykam, and A. Maluckov, "Nonlinear symmetry breaking of Aharonov-Bohm cages," *Phys. Rev. A*, vol. 99, no. 1, 2019, Art. no. 013826.

[146] M. Di Liberto, S. Mukherjee, and N. Goldman, "Nonlinear dynamics of Aharonov-Bohm cages," *Phys. Rev. A*, vol. 100, no. 4, 2019, Art. no. 043829.

[147] M. Creutz, "End states, ladder compounds, and domain-wall fermions," *Phys. Rev. Lett.*, vol. 83, no. 13, pp. 2636−2639, 1999.

[148] N. Chang, *et al*., "Nonlinear Bloch wave dynamics in photonic Aharonov−Bohm cages," *APL Photonics*, vol. 6, no. 3, 2021, Art. no. 030801.

[149] D. E. Chang, V. Vuletic, and M. D. Lukin, "Quantum nonlinear optics − photon by photon," *Nat. Photonics*, vol. 8, no. 9, pp. 685−694, 2014.

[150] A. Zhao and S.-Q. Shen, "Quantum anomalous Hall effect in a flat band ferromagnet," *Phys. Rev. B*, vol. 85, no. 8, 2012, Art. no. 085209.

[151] S. Takayoshi, H. Katsura, N. Watanabe, and H. Aoki, "Phase diagram and pair Tomonaga-Luttinger liquid in a Bose-Hubbard model with flat bands," *Phys. Rev. A*, vol. 88, no. 6, 2013, Art. no. 063613.

[152] W.-F. Tsai, C. Fang, H. Yao, and J. Hu, "Interaction-driven topological and nematic phases on the Lieb lattice," *New J. Phys.*, vol. 17, no. 5, 2015, Art. no. 055016.

[153] M. Metcalf, G. W. Chern, M. D. Ventra, and C. C. Chien, "Matter-wave propagation in optical lattices: geometrical and flat-band effects," *J. Phys. B: At., Mol. Opt. Phys.*, vol. 49, no. 7, 2016, Art. no. 075301.

[154] M. Bercx, J. S. Hofmann, F. F. Assaad, and T. C. Lang, "Spontaneous particle-hole symmetry breaking of correlated fermions on the Lieb lattice," *Phys. Rev. B*, vol. 95, no. 3, 2017, Art. no. 035108.

[155] C. Danieli, A. Andreanov, and S. Flach, "Many-body flatband localization," *Phys. Rev. B*, vol. 102, no. 4, 2020, Art. no. 041116.

[156] I. Vakulchyk, C. Danieli, A. Andreanov, and S. Flach, "Heat percolation in many-body flat-band localizing systems," *Phys. Rev. B*, vol. 104, no. 14, 2021, Art. no. 144207.

[157] Y. Kuno, T. Orito, and I. Ichinose, "Flat-band many-body localization and ergodicity breaking in the Creutz ladder," *New J. Phys.*, vol. 22, no. 1, 2020, Art. no. 013032.

[158] T. Orito, Y. Kuno, and I. Ichinose, "Nonthermalized dynamics of flat-band many-body localization," *Phys. Rev. B*, vol. 103, no. 6, p. L060301, 2021.

[159] C. Danieli, A. Andreanov, and S. Flach, "Many-body localization transition from flat-band fine tuning," *Phys. Rev. B*, vol. 105, no. 4, p. L041113, 2022.

[160] J. Schulenburg, A. Honecker, J. Schnack, J. Richter, and H. J. Schmidt, "Macroscopic magnetization jumps due to independent magnons in frustrated quantum spin lattices," *Phys. Rev. Lett.*, vol. 88, no. 16, 2002, Art. no. 167207.

[161] R. Okuma, *et al*., "Magnon crystallization in the kagome lattice antiferromagnet," *Nat. Commun.*, vol. 10, no. 1, p. 1229, 2019.

[162] J. Schnack, J. Schulenburg, A. Honecker, and J. Richter, "Magnon crystallization in the kagome lattice antiferromagnet," *Phys. Rev. Lett.*, vol. 125, no. 11, 2020, Art. no. 117207.

[163] O. Hart, G. De Tomasi, and C. Castelnovo, "From compact localized states to many-body scars in the random quantum comb," *Phys. Rev. Res.*, vol. 2, no. 4, 2020, Art. no. 043267.

[164] Y. Kuno, T. Mizoguchi, and Y. Hatsugai, "Flat band quantum scar," *Phys. Rev. B*, vol. 102, no. 24, 2020, Art. no. 241115.

[165] T. Simon, M. Daumann, and T. Dahm, "Nearest neighbour particle-particle interaction in fermionic quasi one-dimensional flat band lattices," *Z. Naturforsch. A*, vol. 75, no. 5, pp. 393−402, 2020.

[166] Y. Kuno, T. Mizoguchi, and Y. Hatsugai, "Multiple quantum scar states and emergent slow thermalization in a flat-band system," *Phys. Rev. B*, vol. 104, no. 8, 2021, Art. no. 085130.

[167] Y. Kuno, T. Mizoguchi, and Y. Hatsugai, "Interaction-induced doublons and embedded topological subspace in a complete flat-band system," *Phys. Rev. A*, vol. 102, no. 6, 2020, Art. no. 063325.

[168] C. Lee, A. Rai, C. Noh, and D. G. Angelakis, "Probing the effect of interaction in Anderson localization using linear photonic lattices," *Phys. Rev. A*, vol. 89, no. 2, 2014, Art. no. 023823.

[169] Y. Xing, X. Zhao, Z. Lü, S. Liu, S. Zhang, and H. F. Wang, "Observing two-particle Anderson localization in linear disordered photonic lattices," *Opt. Express*, vol. 29, no. 24, pp. 40428−40446, 2021.

[170] I. I. Yusipov, T. V. Laptyeva, A. Y. Pirova, I. B. Meyerov, S. Flach, and M. V. Ivanchenko, "Quantum subdiffusion with two- and three-body interactions," *Eur. Phys. J. B*, vol. 90, no. 4, p. 66, 2017.

[171] K. Swaminathan, P. Tadros, and S. Peotta, "Signatures of many-body localization of quasiparticles in a flat band superconductor," *Phys. Rev. Res.*, vol. 5, no. 4, 2023, Art. no. 043215.

[172] A. Amo and J. Bloch, "Exciton-polaritons in lattices: a non-linear photonic simulator," *C. R. Phys.*, vol. 17, no. 8, pp. 934−945, 2016.

[173] F. Baboux, *et al*., "Bosonic condensation and disorder-induced localization in a flat band," *Phys. Rev. Lett.*, vol. 116, no. 6, 2016, Art. no. 066402.

[174] O. Jamadi, *et al*., "Reconfigurable photon localization by coherent drive and dissipation in photonic lattices," *Optica*, vol. 9, no. 7, pp. 706−712, 2022.

[175] A. Szameit, *et al*., "Discrete nonlinear localization in femtosecond laser written waveguides in fused silica," *Opt. Express*, vol. 13, no. 26, pp. 10552−10557, 2005.

[176] S. Mukherjee and M. C. Rechtsman, "Observation of Floquet solitons in a topological bandgap," *Science*, vol. 368, no. 6493, pp. 856−859, 2020.

[177] L. J. Maczewsky, *et al*., "Nonlinearity-induced photonic topological insulator," *Science*, vol. 370, no. 6517, pp. 701−704, 2020.

[178] Q. Fu, *et al*., "Optical soliton formation controlled by angle twisting in photonic moiré lattices," *Nat. Photonics*, vol. 14, no. 11, pp. 663−668, 2020.

[179] A. Szameit, *et al*., "Polychromatic dynamic localization in curved photonic lattices," *Nat. Phys.*, vol. 5, no. 4, pp. 271−275, 2009.

[180] C. Martijn de Sterke, A. F. J. Runge, D. D. Hudson, and A. Blanco-Redondo, "Pure-quartic solitons and their generalizations — theory and experiments," *APL Photonics*, vol. 6, no. 9, 2021, Art. no. 091101.

[181] D. Smirnova, *et al*., "Room-temperature lasing from nanophotonic topological cavities," *Light: Sci. Appl.*, vol. 9, no. 1, p. 127, 2020.

[182] L. Yang, G. Li, X. Gao, and L. Lu, "Topological-cavity surface-emitting laser," *Nat. Photonics*, vol. 16, no. 4, pp. 279−283, 2022.

[183] R. Contractor, *et al*., "Scalable single-mode surface-emitting laser via open-Dirac singularities," *Nature*, vol. 608, no. 7924, pp. 692−698, 2022.

[184] J. Ma, *et al*., "Room-temperature continuous-wave topological Dirac-vortex microcavity lasers on silicon," *Light: Sci. Appl.*, vol. 12, no. 1, p. 255, 2023.

[185] Y. Ota, *et al*., "Active topological photonics," *Nanophotonics*, vol. 9, no. 3, pp. 547−567, 2020.

[186] F. Sgrignuoli, M. Röntgen, C. V. Morfonios, P. Schmelcher, and L. Dal Negro, "Compact localized states of open scattering media: a graph decomposition approach for an ab initio design," *Opt. Lett.*, vol. 44, no. 2, pp. 375−378, 2019.

[187] J. Mur-Petit and R. A. Molina, "Van Hove bound states in the continuum: localized subradiant states in finite open lattices," *Phys. Rev. B*, vol. 10, no. 18, 2020, Art. no. 184306.

[188] T. X. Hoang, D. Leykam, and Y. Kivshar, "Photonic flatband resonances in multiple light scattering," *Phys. Rev. Lett.*, vol. 132, no. 4, 2024, Art. no. 043803.

[189] Yi Yang, *et al*., "Photonic flatband resonances for free-electron radiation," *Nature*, vol. 613, no. 7942, pp. 42−47, 2023.

[190] A. Aspuru-Guzik and P. Walther, "Photonic quantum simulators," *Nat. Phys.*, vol. 8, no. 4, pp. 285−291, 2012.

[191] N. A. Olekhno, *et al*., "Topological edge states of interacting photon pairs emulated in a topolectrical circuit," *Nat. Commun.*, vol. 11, no. 1, p. 1436, 2020.

[192] D. Yu, G. Li, L. Wang, D. Leykam, L. Yuan, and X. Chen, "Moiré lattice in one-dimensional synthetic frequency dimension," *Phys. Rev. Lett.*, vol. 130, no. 14, 2023, Art. no. 143801.

[193] G. Li, *et al*., "Observation of flat-band and band transition in the synthetic space," *Adv. Photonics*, vol. 4, no. 3, 2022, Art. no. 036002.

[194] A. R. Kolovsky, P. S. Muraev, and S. Flach, "Conductance transition with interacting bosons in an Aharonov-Bohm cage," *Phys. Rev. A*, vol. 108, no. 1, p. L010201, 2023.

[195] J. G. C. Martinez, C. S. Chiu, B. M. Smitham, and A. A. Houck, "Flat-band localization and interaction-induced delocalization of photons," *Sci. Adv.*, vol. 9, no. 50, 2023, Art. no. eadj7195.